Heliyon 10 (2024) e37829

Contents lists available at ScienceDirect

Heliyon

journal homepage: www.cell.com/heliyon

Research article

Targeted degradation of specific TEAD paralogs by small molecule degraders

Hui Chen [b,1], Artem Gridnev [a,c,1], Netanya Schlamowitz [a,d], Wanyi Hu [b], Kuntala Dey [b], Guangrong Zheng [b,**], Jyoti R. Misra [a,*]

[a] Department of Pharmacological Sciences, Stony Brook University School of Medicine, Stony Brook, 11794, USA
[b] Department of Medicinal Chemistry, College of Pharmacy, University of Florida, Gainesville, FL, 32610, USA
[c] Graduate School of Biomedical Sciences, Oregon Health & Sciences University, Portland, OR, USA
[d] Graduate School of Biomedical Sciences, University of Texas Southwestern Medical Center, Dallas, TX, USA

A B S T R A C T

The transcription factors, TEAD1-4 together with their co-activator YAP/TAZ function as key downstream effectors of the Hippo pathway. Hyperactivation of TEAD-YAP/TAZ activity is observed in many human cancers. TEAD1-4 possess distinct physiological and pathological functions, with conserved sequences and structures. Targeting specific isoforms within TEAD1-4 can serve as valuable chemical probes for investigating TEAD-related functions in both development and diseases. We report the TEAD-targeting proteolysis targeting chimera (PROTAC), **HC278**, which achieves effective and specific targeting of TEAD1 and TEAD3 at low nanomolar doses while weakly degrading TEAD2 and TEAD4 at higher doses. Proteomic analysis of >6000 proteins confirmed their highly selective TEAD1 and TEAD3 degradation. Consistently, **HC278** can suppress the proliferation of YAP-dependent NCI-H226 mesothelioma cells. Mechanistic exploration revealed that both CRBN and proteasome systems are involved in the TEAD degradation induced by **HC278**. Moreover, RNA-seq and Gene Set Enrichment Analysis (GSEA) revealed that the YAP signature genes such as CTGF, CYR61, and ANKRD1 are significantly downregulated by **HC278** treatment. Overall, **HC278** serves as a valuable chemical tool for unraveling the intricate biological roles of TEAD1 and TEAD3 and holds the potential as a lead compound for developing targeted therapy for TEAD1/3-driven pathologies.

1. Introduction

The paralogous transcriptional coactivators Yes-associated Protein (YAP) and transcriptional activator with PDZ binding motif (TAZ) function as the distal effectors of the Hippo signaling pathway, acting as oncogenic drivers in many cancers including, mesothelioma, glioma, meningioma, and cancers of the lung, liver, and thyroid [1–4]. The regulatory mechanism of YAP and TAZ involves their subcellular localization, inactive when in the cytoplasm but becomes active within the nucleus. This activity is controlled by their phosphorylation status, which is governed by the Hippo signaling pathway. This pathway is a well-conserved kinase cascade comprising of mammalian STE20-like kinases 1/2 (MST1/2), large tumor suppressor kinases 1/2 (LATS1/2), and their associated scaffold/adaptor proteins, Salvador Homolog (SAV1) and Mob 1 Homolog (MOB1). The SAV1-MST1/2 complex phosphorylates and activates the LATS1/2-MOB1 complex. Once activated, LATS1/2 in turn phosphorylates YAP/TAZ, leading to their cytoplasmic retention and subsequent degradation. However, when the Hippo pathway is dysregulated, hypo/unphosphorylated YAP/TAZ translocates into the nucleus, where it associates with several transcription factors such as TEA Domain transcription factors

* Corresponding author.
** Corresponding author.
E-mail addresses: Zhengg@cop.ufl.edu (G. Zheng), jyoti.misra@stonybrook.edu (J.R. Misra).
[1] These authors contributed equally.

https://doi.org/10.1016/j.heliyon.2024.e37829
Received 20 March 2024; Received in revised form 6 September 2024; Accepted 10 September 2024
Available online 14 September 2024

(TEAD1-4), SMAD family member 3 (SMAD3), and runt-related transcription factor 1 (RUNX1) to induce the transcription of genes encoding pro-proliferative and anti-apoptotic factors [5,6]. Of these, TEAD1-4 regulate the majority of YAP target genes.

Large scale analysis of human cancer samples has revealed that multiple Hippo pathway genes are mutated in a wide range of cancer types [7]. Although genetic alterations in the Hippo pathway components are rare in most cancer types, they are frequently observed in select cancers such as mesothelioma, meningioma, and squamous cell cancers [7,8]. In addition, non-genetic dysregulation of the upstream regulatory components can also lead to increased YAP nuclear localization and transcriptional activity [9–11]. Numerous studies have established that YAP/TAZ plays an oncogenic role by promoting cancer cell proliferation, survival, cancer stem cell fate, and resistance to chemotherapy and targeted therapy [12,13]. In addition, YAP directly promotes programmed death-ligand 1 (PD-L1) expression and contributes to resistance to immune checkpoint inhibitors [14–16]. Thus, YAP/TAZ provides a critical point for therapeutic intervention. However, YAP/TAZ is intrinsically disordered and therefore difficult to be targeted therapeutically. Since YAP must associate with TEAD1-4 to exert its oncogenic transcriptional activity, its activity can be indirectly controlled through TEAD.

The TEAD transcription factors exist in four isoforms that exhibit a high degree of sequence conservation [17,18]. They undergo autopalmitoylation at a conserved cysteine residue, and the covalently attached palmitic acid occupies a hydrophobic central pocket [19,20]. Small molecules that occupy this pocket and inhibit TEAD autopalmitoylation impair TEAD stability and allosterically inhibit YAP-TEAD interaction [21,22]. A number of such molecules have been developed and exhibit significant anticancer activity in pre-clinical and Phase I clinical trials [20,23–39]. However, some cancers develop resistance through association of TEAD with the transcriptional corepressors vestigial like family member 3 (VGLL3) [40]. Thus, targeted degradation of TEAD could potentially overcome this problem [41].

Proteolysis targeting chimeras (PROTACs) have emerged as a new frontier in drug discovery, especially for difficult oncogenic targets [42–48]. PROTACs are heterobifunctional molecules that consist of two different moieties, one binding to the target protein and the other binding to an E3 ubiquitin ligase [49,50]. They bring the target protein in close proximity to the E3 ligase and promote their ubiquitination and subsequent degradation by the proteasomal machinery [51,52]. As opposed to traditional inhibitors that act through occupancy-driven pharmacology, PROTACs act through event-driven pharmacology and function catalytically to degrade multiple copies of the target protein [53–55]. Thus, PROTACs have the potential to be superior when compared to traditional inhibitors. Moreover, in many instances, PROTACs are more selective than the inhibitors because they must form a productive ternary complex between the target protein and the E3 ligase [56,57]. Additionally, while an inhibitor-bound target protein can still bind to its partners in a protein complex, PROTACs induce destabilization of the whole protein complexes by degrading their targets [58,59]. Collectively, PROTACs afford several advantages over inhibitors and several oncoprotein-targeting PROTACs have been advanced to clinical trials [53,60].

Here we report the development of TEAD-degrading PROTACs that induce degradation of specific isoforms of TEAD by engaging the Cullin–RING ubiquitin ligase complex 4 (CRL4)-cereblon (CRBN) E3 ligase and proteasome. They potently degrade TEAD1 and TEAD3 at low nanomolar doses and weakly degrade TEAD2 and TEAD4 at higher doses. Proteomic analyses and Western blotting confirmed that they potently and specifically degrade TEAD1, TEAD3, and to a lesser extent TEAD2 and TEAD4. Moreover, transcriptomic analyses revealed that they cause downregulation of YAP transcriptional targets. Consistently, they inhibit the proliferation of YAP-driven NCI-H226 mesothelioma cancer cells.

2. Materials and methods

2.1. Cell lines and cell line culture

HEK293 (ATCC, (RRID: CVCL_0045), NCI-H226 (NCI, (RRID: CVCL_1544) and NCI-H28 (NCI, (RRID: CVCL_1555), cells were cultured in Dulbecco's modified Eagle's Medium (DMEM, Corning Cat. #10-013-CV) supplemented with 10 % heat-inactivated fetal bovine serum (HI FBS, Gibco™ Cat. #10438026) and 1 % antibiotic/antimycotic (Gibco™). All cell lines were tested to be mycoplasma free. All cells were cultured in a humidified incubator at 37 °C with 5 % CO_2. HEK293-PanTEAD cells were created by stable transfection of HEK293 cells with lentivirus containing pTRE-Puro-PanTEAD construct and were maintained in DMEM supplemented with 10 % FBS, 1 % antibiotic/antimycotic, and 2.5 μg ml of puromycin.

2.2. Molecular biology

To make pCDNA3.1-pan-TEAD, cDNAs for full-length TEAD1/2/3/4 were PCR amplified with forward primers containing sequences for FLAG, Myc, HA, and V5 epitope tags and sequences for T2A, P2A and E2A and cloned simultaneously into the *Bam*HI and XbaI site in pCDNA3.1 using NEBuilder® HiFi DNA Assembly Kit (New England Biolabs Cat. #E2621). To make pTRE-Puro-pan-TEAD, the entire cassette containing all the TEAD was amplified from pCDNA3.1-pan-TEAD and cloned between MluI and AgeI in pTRE by NEBuilder® HiFi DNA Assembly. To make pGEX-3X-TEAD1-YBD-C359A, pGEX-3X-TEAD2-YBD-C380A, pGEX-3X-TEAD3-YBD-C368A, pGEX-3X-TEAD4-YBD-C367A, the coding sequences for YBD of TEAD1-4 were PCR amplified from pCMX-GAL4-TEAD1 (Addgene #33108), pCMX-GAL4-TEAD2 (Addgene #33107), pCMX-GAL4-TEAD3 (Addgene #33106), pCMX-GAL4-TEAD4 (Addgene #33105), pRK5-Myc-TEAD4 (Addgene #24638), as two overlapping fragments with the mutations introduced in the primers for amplifying them, and cloned into the BamH1 site in PGEX-3X plasmid by NEBuilder® HiFi DNA Assembly.

2.3. Lentivirus production

HEK293 cells were seeded in antibiotic-free medium at a density of 5×10^5 cells per well of a 6-well dish and allowed to attach overnight. Cells were transfected with packaging plasmids psPAX2 and pMD2. G along with the transfer plasmid pTRE-puro-pan-TEAD. After 48 h virus supernatants were collected and filtered through a 0.45 μm syringe filter. 4× lentivirusmaity concentration solution (40 % w/v PEG-8000, 1.2 M NaCl in 1× PBS, pH 7.4) was added at a 1:4 to the filtered supernatant and the mixture was rotated end-over-end overnight at 4 °C. The following day, the virus was precipitated by centrifugation at 1600×*g* for 60 min at 4 °C and diluted in 1× PBS. Virus aliquots were stored at −80 °C.

2.4. Stable cell line generation

Lentiviral particles were used to transduce HEK293 cells. 8 μg/mL polybrene was added to antibiotic-free medium containing the viruses to enhance transduction efficiency. Stable clones were established by selection with 2.5 μg/mL puromycin starting 48 h after transduction until distinct colonies formed. Colonies were isolated and screened for expression of epitope-tagged TEAD paralogues by western blotting.

2.5. Clonogenic assay

Clonogenic assays were done as previously described [24]. Briefly, an equal number NCI-H226 cells were plated in triplicate and were treated with DMSO or different doses of **HC278** for two weeks, following which they were fixed with 4 % PFA and stained with 0.5 % crystal violet dissolved in methanol. The images were acquired using Gelcount (Oxford Optronix) mammalian-cell colony, spheroid, and organoid counter, and the colony areas were quantified using FIJI.

2.6. Western blotting

For detection of endogenous TEAD in cells, NCI-H226 cells plated at a density of 2×10^5 cells per well of a 6-well dish were harvested by trypsinization after treatment. Cell pellets were lysed in 100 μL of RIPA buffer on ice for 30 min and sonicated at 50 % amplitude for 5 s. Samples were centrifuged at 18213×*g* for 20 min at 4 °C to remove cell debris. Supernatants were diluted 2× Laemmli buffer, boiled at 98 °C for 5 min, and resolved by SDS-PAGE. Gels were transferred to nitrocellulose membranes using a Bio-RAD Trans-Blot Turbo semi-dry transfer system. After blocking with protein-free blocking buffer (Li-COR), blots were incubated overnight at 4 °C with primary antibodies against TEAD1 (D9X2L, Cell Signaling Technology #12292, 1:750), TEAD2 (C-10, Santa Cruz # sc-518181, 1:1000), TEAD3 (Abcam #ab138246 1:1000), and TEAD4 (5H3, Abcam #ab58310 1:5000), following which, they were washed thrice with TBST buffer and incubated with appropriate IR Dye 680 or IR Dye 780 conjugated secondary antibodies at room temperature for 2 h. Subsequently, the blots were washed thrice with TBST and scanned with a Li-COR Odyssey CLx imager. Overexpressed TEAD in HEK293-pTRE-puro-pan-TEAD was conducted as previously described, except that cells were seeded at 1.2-1.5 $\times 10^5$ cells per well of a 24-well dish and paralogues detected by antibodies against FLAG (1:5000), Myc (1: 5000), HA (1:2000), V5 (1:5000) tags.

2.7. RNA extraction and RT-qPCR

MDA-MB-231 cells were seeded at ~50 % confluence in 6 well dishes and allowed to attach overnight. Cells were then treated with DMSO or different doses of **HC278** (500 nM and 1 μM) for 24 h. Total RNA was extracted with TRIzol reagent (Invitrogen), following the manufacturer's protocol. 1 μg of total RNA was reverse transcribed to cDNA using the iScript™ gDNA Clear cDNA synthesis kit (Bio-RAD). qPCR was performed with Applied Biosystems Fast SYBR Green master mix on an Applied Biosystems QuantStudio 6 Flex system. Target genes were normalized to GAPDH mRNA levels and relative fold changes were calculated as $2^{-\Delta\Delta Ct}$.

2.8. Protein purification

Recombinant GST-tagged TEAD1-4 YBD with the conserved cysteine mutated to alanine (CS mutants) were purified from *E. coli*. BL-21(DE3) cells were transformed with pGEX-3X-TEAD1-YBD, pGEX-3X-TEAD2-YBD, pGEX-3X-TEAD3-YBD, pGEX-3X-TEAD4-YBD plasmids. Cultures were grown to 0.6 OD 600 nm and protein production was induced by 300 μM IPTG, at 16 °C overnight. Cells were collected by centrifuging at 8000 rpm for 10 min and were resuspended in ice-cold lysis buffer (50 mM TRIS pH 7.4, 1 mM EDTA, 150 mM NaCl, 1 mM DTT) supplemented with protease inhibitor cocktail, 0.1 % triton X 100 and Lysozyme, and lysed using sonication and a homogenizer. The soluble fraction was separated by centrifuging at 20,000 rpm for 30 min at 4°C and was incubated with Glutathione Sepharose 4B affinity resin for 2 h. After thorough washing, the protein was eluted with 10 mM glutathione and dialyzed overnight. The purity was verified with SDS-PAGE and Coomassie Brilliant Blue staining.

2.9. AlphaLISA assay for evaluating the ternary complex formation

AlphaLISA assay was used to evaluate the in vitro ternary complex formation between potential target proteins (GST-tagged TEAD1-4), PROTAC, and CRBN/DDB1 complex (His-tagged CRBN/DDB1 complex). Assays were performed at room temperature. All

reagents were diluted in an assay buffer of 50 mM HEPES, pH 7.5, 150 mM NaCl, 0.1 % BSA, and 0.005 % Tween 80. To a 96-well PCR plate were added 10 μL of 6 × His-tagged protein (CRBN/DDB1, 100 nM), 10 μL of the serially diluted compound solution (4 × dilution), and 10 μL of GST-TEAD1-4 (100 nM). After incubating at room temperature for 60 min, 5 μL of alpha glutathione donor beads (160 μg/mL, Cat. No. 6765300, PerkinElmer) and 5 μL of anti-6 × His acceptor beads (160 μg/mL, Cat. No. AL128A, PerkinElmer) were added to each well under subdued light, successively. Then, the resulting mixture was transferred to two adjacent wells (17 μL each) of a 384-well white OptiPlate (Cat. No. 6008280, PerkinElmer), and incubated for an additional 18 h in the dark. The luminescence signal was detected on a Biotek's Synergy Neo 2 multimode plate reader installed with an AphaScreen filter cube. Intensity values were plotted in GraphPad Prism with PROTAC concentration values represented on a log 10 scale.

2.10. Proteomic analysis

NCI-H226 cells were treated in triplicate with either DMSO or 500 nM **HC278** for 24 h, following which, the cells were trypsinized and collected by centrifugation. The cell pellets were lysed in RIPA buffer and 15 μL of each sample was diluted to 50 μL with 5 % SDS, 100 mM triethylammonium bicarbonate (TEAB). 2 μL of 500 mM (tris(2-carboxyethyl) phosphine) (TCEP) was added to reduce disulfide bonds and samples were incubated at 56 °C for 30 min. After cooling, 2 μL of 500 mM iodoacetamide (IAA) was added to alkylate the free cysteine thiols, and samples were incubated for 30 min at room temperature in the dark. Samples were then digested overnight with trypsin at 37 °C using an S-Trap (Protifi). Following digestion, the peptides were eluted from the S-Trap, dried, and reconstituted in 75 μL of 50 mM TEAB was added. The samples were labeled with TMT-6 plex reagents, quenched with 5 % hydroxylamine, and combined. A high-pH reverse-phase fractionation spin column (Pierce) was used according to the manufacturer's directions to fractionate the sample into 8 fractions. The fractions were dried in a SpeedVac and reconstituted in a 2 % acetonitrile, 0.1 % TFA buffer.

Peptides were analyzed on a Thermo Orbitrap Eclipse MS system coupled to an Ultimate 3000 RSLC-Nano liquid chromatography system. Samples were injected onto a 75 μm i. d., 75-cm long EasySpray column (Thermo) and eluted with a gradient from 0 to 28 % buffer B over 180 min at a flow rate of 250 nL/min. Buffer A contained 2 % (v/v) ACN and 0.1 % formic acid in water, and buffer B contained 80 % (v/v) ACN, 10 % (v/v) trifluoroethanol, and 0.1 % formic acid in water. at a flow rate of 250 nL/min. Spectra were continuously acquired in a data-dependent manner throughout the gradient, acquiring a full scan in the Orbitrap (at 120,000 resolution with a standard AGC target) followed by MS/MS scans on the most abundant ions in 2.5 s in the ion trap (turbo scan type with an intensity threshold of 5,000, CID collision energy of 35 %, standard AGC target, maximum injection time of 35 ms and isolation width of 0.7 m/z). Charge states from 2 to 6 were included. Dynamic exclusion was enabled with a repeat count of 1, an exclusion duration of 25 s and an exclusion mass width of ±10 ppm. Real-time search was used for selection of peaks for SPS-MS3 analysis, with searched performed against the human reviewed protein database from UniProt, Up to 1 missed tryptic cleavage was allowed, with carbamidomethylation (+57.0215) of cysteine and TMT reagent (+229.1629) modification of lysine and peptide N-termini used as static modifications, and oxidation (+15.9949) of methionine used as a variable modification. MS3 data were collected for up to 10 MS2 peaks which matched to fragments from the real-time peptide search identification, in the orbitrap at a resolution of 50,000, HCD collision energy of 65 % and a scan range of 100–500.

Protein identification and quantification were done using Proteome Discoverer v.3.0 SP1 (Thermo). Raw MS data files were analyzed against the human reviewed protein database from UniProt. Both Comet and Sequest HT with INFERYS Rescoring were used, with carbamidomethylation (+57.0215) of cysteine and TMT reagent (+229.1629) of lysine and peptide N-termini used as static modifications and oxidation (+15.9949) of methionine used as a variable modification. Reporter ion intensities were reported, with further normalization performed by using the total intensity in each channel to correct discrepancies in sample amount in each channel. The false-discovery rate (FDR) cutoff was 1 % for all peptides.

2.11. RNA-seq experiment

NCI-H226 cells were treated in triplicate with either DMSO or 500 nM **HC278** for 24 h, following which, the cells were trypsinized and collected by centrifugation. Total RNA was extracted with TRIzol reagent (Invitrogen) with on-column DNA removal. The RNA sequencing library was prepared using Illumina Stranded mRNA prep kit (20040532) according to Manufacturer's protocol. This protocol requires input RNA with RIN (RNA integrity number) > 7 RNA and concentration range between 25 ng and 1000 ng. Illumina UMI barcodes were used to multiplex the libraries as per the Manufacturer's instructions. The quality and quantity of each sequencing final library were assessed using Agilent 2100 BioAnalyzer system (Agilent, CA, USA). A total of 10 nM Picogreen measured library were pooled for 1.3 pM loading on the sequencer. The pooled libraries were sequenced on Illumina NexSeq platform in SE75 (75 bp single end) run with the NextSeq reagent kit v2.5 for 75 cycles. About 30–40 Million sequencing reads were generated per sample for the transcriptome analysis. Single end demultiplexed fastq files were generated using bcl2fastq2 (Illumina, v2.17), from NextSeq 550 v2.5 reagent's bcl files. Initial quality control was performed using FastQC v0.11.8 and multiqc v1.7. Fastq files were imported batch wise, trimmed for adapter sequences followed by quality trimming using CLC Genomics Workbench (CLC Bio, v23.0.3). The imported high-quality reads were mapped against gene regions and transcripts annotated by ENSEMBL v99 hg38 using the RNA-Seq Analysis tool v2.7 (CLC Genomics Workbench), only matches to the reverse strand of the genes were accepted (using the strand-specific reverse option). Differential gene expression analysis between the sample groups was done using the Differential Expression for RNA-seq tool v2.8, where the normalization method was set as TMM. Differential expression between the groups was tested using a control group, outliers were downweighed, and filter on average expression for FDR correction was enabled.

2.12. Quantification and statistical analysis

Results were recorded and sorted in Microsoft Excel and all statistical analyses were performed using GraphPad Prism (San Diego, CA). Histograms show the mean plus Standard Error of Mean (SEM). For pairwise comparisons two-tailed Student's *t*-test was used for parametric distributions and a Mann-Whitney test was used for non-parametric distributions.

2.13. Chemistry methods

2.13.1. General methods

DMF and DCM were obtained via a solvent purification system by filtering through two columns packed with activated alumina and 4 Å molecular sieve, respectively. Water was purified with a Milli-Q Simplicity 185 Water Purification System (Merck Millipore). All other chemicals and solvents obtained from commercial suppliers were used without further purification. Flash chromatography was performed using silica gel (230–400 mesh) as the stationary phase. Reaction progress was monitored by thin-layer chromatography (silica-coated glass plates) and visualized by 256 nm and 365 nm UV light, and/or by LC-MS. ^{1}H NMR spectra were recorded in $CDCl_3$, CD_3OD, or DMSO-d_6 at 600 MHz, and ^{13}C NMR spectrum was recorded at 150 MHz using a Bruker (Billerica, MA) DRX Nuclear Magnetic Resonance (NMR) spectrometer. ^{1}H and ^{13}C spectra are internally referenced to residual solvent signals ($CDCl_3$, δ 7.26, 77.16; CD_3OD, δ 3.31, 49.00; DMSO-d_6, δ 2.50, 39.52.). Data for ^{1}H is reported as follows: chemical shift (δ ppm), multiplicity (s = singlet, d = doublet, t = triplet, q = quartet, m = multiplet), coupling constant (Hz), integration. All final compounds for biological testing were of ≥95.0 % purity as analyzed by ^{1}H NMR. High resolution mass spectra (HRMS) were recorded on an Agilent 6230 Time-of-Flight (TOF) mass spectrometer.

Methyl 2-(3-cyanophenyl)acetate (**17**). To a solution of methyl 2-(3-bromophenyl)acetate **16** (2.50 g, 10.91 mmol) and $Zn(CN)_2$ (0.83 g, 7.09 mmol) in DMF (30 mL) was added $Pd(PPh_3)_4$ (0.63 g, 0.55 mmol). The resulting mixture was stirred at 90 °C for 4 h under N_2 atmosphere. After completion of the reaction by checking the thin layer chromatography, the mixture was quenched by adding aqueous 2 N ammonia and extracted with EtOAc. The combined organic layers were washed with brine and then concentrated. The residue was purified by flash column chromatography (0 %–15 % of EtOAc in hexanes) to afford compound **17** (1.50 g, 79 % yield) as a white solid. ^{1}H NMR (600 MHz, Chloroform-*d*) δ 7.60–7.55 (m, 2H), 7.52 (dt, J = 7.9, 1.5 Hz, 1H), 7.44 (t, J = 7.7 Hz, 1H), 3.71 (s, 3H), 3.66 (s, 2H). LRMS (ESI) *m/z*: 177.0 $[M + H]^+$.

Methyl-3-(aminomethyl)phenylacetate hydrochloride (**18**). To a solution of compound **17** (1.40 g, 7.99 mmol) in MeOH (18 mL) and 4 M HCl in dioxane (3 mL) was added 10 % Pd/C (0.14 g). The resulting mixture was stirred at room temperature overnight under H_2 atmosphere. After completion of the reaction by checking the thin layer chromatography, the mixture was filtered over Celite and concentration of the filtrate, the resulting crystals were taken with EtOAc to give compound **18** (0.61 g, 35 % yield) as a gray solid. ^{1}H NMR (600 MHz, Methanol-d_4) δ 7.44–7.33 (m, 4H), 4.11 (s, 2H), 3.71 (s, 2H), 3.69 (s, 3H). LRMS (ESI) *m/z*: 180.0 $[M + H]^+$.

Methyl 5-hydroxy-2-naphthoate (**20**). To a solution of 5-bromo-2-naphthoic acid **19** (10 g, 39.83 mmol) in tetrabutylammonium hydroxide (100 mL, 40 % in H_2O) and deionized water (50 mL) was added Cu_2O (0.85 g, 5.97 mmol), 4,7-dihydroxy-1,1′-phenanthroline (1.94 g, 9.16 mmol). The resulting mixture was stirred at 100 °C overnight under N_2 atmosphere. After completion of the reaction by checking the thin layer chromatography, the mixture was acidified to pH 2–3 with 2 N HCl after cooling to room temperature. The mixture was extracted with EtOAc. The combined organic layers were washed with brine, then dried over Na_2SO_4, filtered, and concentrated. The resulting residue was used directly without purification. To a solution of the above residue in MeOH (150 mL) was added $SOCl_2$ (47.35 g, 398.02 mmol). The resulting mixture was stirred at 70 °C for 2 h. After completion of the reaction by checking the thin layer chromatography, the mixture was concentrated directly and extracted with EtOAc. The combined organic layers were washed with brine and then concentrated. The residue was purified by flash column chromatography (0 %–20 % of EtOAc in hexanes) to afford compound **20** (3.83 g, 48 % yield for two steps) as a colorless oil. ^{1}H NMR (600 MHz, DMSO-d_6) δ 10.37 (s, 1H), 8.52 (d, J = 1.7 Hz, 1H), 8.24–8.20 (m, 1H), 7.91 (dd, J = 8.8, 1.7 Hz, 1H), 7.57–7.52 (m, 1H), 7.41 (t, J = 7.9 Hz, 1H), 7.01 (dd, J = 7.6, 1.0 Hz, 1H), 3.91 (s, 3H).

Methyl 5-(4-(trifluoromethyl)phenoxy)-2-naphthoate (**22**). To a solution of compound **20** (3 g, 14.84 mmol) and 1-bromo-4-(trifluoromethyl)benzene **21** (4.01 g, 17.80 mmol) in toluene (60 mL) was added $Pd(OAc)_2$ (0.16 g, 0.74 mmol), tBu-XPhos (0.44 g, 1.04 mmol), and K_3PO_4 (6.30 g, 29.67 mmol). The resulting mixture was stirred at 110 °C overnight under N_2 atmosphere. After completion of the reaction by checking the thin layer chromatography, the mixture was filtered and concentrated. The residue was purified by flash column chromatography (0 %–5 % of EtOAc in hexanes) to afford compound **22** (3.82 g, 74 % yield) as a colorless oil. ^{1}H NMR (600 MHz, Chloroform-*d*) δ 8.66 (d, J = 1.6 Hz, 1H), 8.13 (d, J = 8.8 Hz, 1H), 8.07 (dd, J = 8.8, 1.6 Hz, 1H), 7.82 (d, J = 8.2 Hz, 1H), 7.62–7.56 (m, 2H), 7.51 (t, J = 7.9 Hz, 1H), 7.17 (dd, J = 7.6, 1.0 Hz, 1H), 7.08 (d, J = 8.6 Hz, 2H), 4.00 (s, 3H).

5-(4-(trifluoromethyl)phenoxy)-2-naphthoic acid (**23**). To a solution of compound **22** (2.80 g, 8.09 mmol) in MeOH (30 mL) and THF (10 mL) was added 2 N NaOH (30 mL). The resulting mixture was stirred at room temperature for 3 h. After completion of the reaction by checking the thin layer chromatography, the mixture was acidified to pH 3–4 with con. HCl. The mixture was extracted with EtOAc. The combined organic layers were washed with brine, then dried over Na_2SO_4, filtered, and concentrated to afford compound **23** (2.50 g, 93 % yield) as a white solid. ^{1}H NMR (600 MHz, DMSO-d_6) δ 13.21 (s, 1H), 8.71 (d, J = 1.6 Hz, 1H), 8.08–8.00 (m, 3H), 7.77–7.71 (m, 2H), 7.64 (t, J = 7.9 Hz, 1H), 7.37 (dd, J = 7.6, 1.0 Hz, 1H), 7.17 (d, J = 8.6 Hz, 2H).

Methyl 2-(3-((5-(4-(trifluoromethyl)phenoxy)-2-naphthamido)methyl)phenyl)acetate (**24**). To a solution of compound **23** (240 mg, 0.72 mmol) in DMF (5 mL) was added DIEA (373.41 mg, 2.89 mmol), HATU (357.03 mg, 0.94 mmol), and compound **18** (156 mg, 0.72 mmol), successively. The resulting mixture was stirred at room temperature overnight. After completion of the reaction by checking the thin layer chromatography, the mixture was extracted with EtOAc. The combined organic layers were washed with brine

and then concentrated. The residue was purified by flash column chromatography (0 %–30 % of EtOAc in hexanes) to afford compound **24** (290 mg, 81 % yield) as a white solid. ^{1}H NMR (600 MHz, Chloroform-*d*) δ 8.38 (d, J = 1.7 Hz, 1H), 8.15–8.10 (m, 1H), 7.85 (dd, J = 8.8, 1.8 Hz, 1H), 7.80–7.75 (m, 1H), 7.62–7.55 (m, 2H), 7.50 (t, J = 7.9 Hz, 1H), 7.37–7.29 (m, 3H), 7.23 (dt, J = 7.3, 1.7 Hz, 1H), 7.14 (dd, J = 7.5, 0.9 Hz, 1H), 7.09–7.05 (m, 2H), 6.58 (t, J = 5.7 Hz, 1H), 4.70 (d, J = 5.6 Hz, 2H), 3.70 (s, 3H), 3.64 (s, 2H). LRMS (ESI) *m/z*: 494.1 $[M + H]^+$.

2-(3-((5-(4-(trifluoromethyl)phenoxy)-2-naphthamido)methyl)phenyl)acetic acid (**25**). To a solution of compound **24** (275 mg, 0.56 mmol) in MeOH (12 mL) and THF (4 mL) was added 2 N NaOH (3 mL). The resulting mixture was stirred at room temperature for 2 h. After completion of the reaction by checking the thin layer chromatography, the mixture was acidified to pH 3–4 with con. HCl. The mixture was extracted with EtOAc. The combined organic layers were washed with brine, then dried over Na_2SO_4, filtered, and concentrated to afford compound **25** (264 mg, 99 % yield) as a white solid. ^{1}H NMR (600 MHz, DMSO-d_6) δ 12.30 (s, 1H), 9.26 (t, J = 6.0 Hz, 1H), 8.61 (t, J = 1.2 Hz, 1H), 8.04–7.98 (m, 2H), 7.96 (d, J = 8.2 Hz, 1H), 7.78–7.70 (m, 2H), 7.63 (t, J = 7.9 Hz, 1H), 7.33 (dd, J = 7.6, 1.0 Hz, 1H), 7.31–7.26 (m, 1H), 7.26–7.21 (m, 2H), 7.19–7.13 (m, 3H), 4.53 (d, J = 5.9 Hz, 2H), 3.55 (s, 2H). LRMS (ESI) *m/z*: 480.1 $[M + H]^+$.

N-(3-(2-((4-((2-(2,6-dioxopiperidin-3-yl)-1,3-dioxoisoindolin-4-yl)amino)butyl)amino)-2-oxoethyl)benzyl)-5-(4-(trifluoromethyl) phenoxy)-2-naphthamide (**1**). To a solution of compound **25** (10 mg, 0.021 mmol) in DMF (0.5 mL) was added DIEA (10.78 mg, 0.083 mmol), HATU (10.31 mg, 0.027 mmol), and 4-((4-aminobutyl)amino)-2-(2,6-dioxopiperidin-3-yl)isoindoline-1,3-dione hydrochloride **26a** (7.94 mg, 0.021 mmol), successively. The resulting mixture was stirred at room temperature overnight. After completion of the reaction by checking the thin layer chromatography, the mixture was extracted with EtOAc. The combined organic layers were washed with brine and then concentrated. The residue was purified by flash column chromatography (0 %–9 % of MeOH in DCM) to afford compound **1** (9.1 mg, 54 % yield) as a yellow solid. ^{1}H NMR (600 MHz, Chloroform-*d*) δ 8.38 (d, J = 1.7 Hz, 1H), 8.21 (s, 1H), 8.13–8.08 (m, 1H), 7.84 (dd, J = 8.8, 1.8 Hz, 1H), 7.78–7.74 (m, 1H), 7.61–7.56 (m, 2H), 7.49 (dd, J = 8.2, 7.6 Hz, 1H), 7.44 (dd, J = 8.5, 7.1 Hz, 1H), 7.36–7.27 (m, 3H), 7.19 (dt, J = 7.1, 1.8 Hz, 1H), 7.13 (dd, J = 7.6, 1.0 Hz, 1H), 7.09–7.03 (m, 3H), 6.82–6.75 (m, 2H), 6.13 (t, J = 5.7 Hz, 1H), 5.58 (t, J = 5.9 Hz, 1H), 4.92–4.86 (m, 1H), 4.73–4.63 (m, 2H), 3.55 (s, 2H), 3.28–3.23 (m, 2H), 3.23–3.17 (m, 2H), 2.89–2.82 (m, 1H), 2.82–2.66 (m, 2H), 2.14–2.07 (m, 1H), 1.57–1.52 (m, 4H). ^{13}C NMR (150 MHz, $CDCl_3$) δ 171.13, 171.07, 169.72, 168.63, 167.69, 167.30, 160.79, 151.72, 146.92, 139.19, 136.32, 135.70, 134.47, 132.56, 132.48, 129.58, 129.01, 128.78, 128.35, 127.81, 127.46 (q, J = 3.7 Hz), 127.09, 126.98, 125.69, 125.41 (q, J = 32.8 Hz), 124.26 (q, J = 271.5 Hz), 124.10, 122.79, 117.90, 116.90, 116.77, 111.75, 110.09, 49.03, 44.19, 43.82, 42.20, 39.25, 31.53, 27.10, 26.52, 22.93. LRMS (ESI) *m/z*: 806.2 $[M + H]^+$. HRMS (ESI): *m/z* calcd for $C_{44}H_{39}F_3N_5O_7^+$ $[M + H]^+$, 806.2801; found, 806.2791.

N-(3-(2-((6-((2-(2,6-dioxopiperidin-3-yl)-1,3-dioxoisoindolin-4-yl)amino)hexyl)amino)-2-oxoethyl)benzyl)-5-(4-(trifluoromethyl) phenoxy)-2-naphthamide (**2**). Compound **2** was synthesized from **25** and **26b** using a similar procedure for the preparation of compound **1**. It was obtained as a white solid (9.2 mg, 53 % yield). ^{1}H NMR (600 MHz, Chloroform-*d*) δ 8.39 (d, J = 1.7 Hz, 1H), 8.18 (s, 1H), 8.11 (d, J = 8.8 Hz, 1H), 7.85 (dd, J = 8.8, 1.8 Hz, 1H), 7.77 (d, J = 8.2 Hz, 1H), 7.61–7.56 (m, 2H), 7.49 (t, J = 7.9 Hz, 1H), 7.46 (dd, J = 8.5, 7.1 Hz, 1H), 7.35–7.27 (m, 3H), 7.19 (dt, J = 7.4, 1.7 Hz, 1H), 7.13 (dd, J = 7.6, 1.0 Hz, 1H), 7.08–7.04 (m, 3H), 6.83 (d, J = 8.5 Hz, 1H), 6.78 (t, J = 5.8 Hz, 1H), 6.18 (t, J = 5.6 Hz, 1H), 5.51 (t, J = 5.9 Hz, 1H), 4.88 (dd, J = 12.4, 5.4 Hz, 1H), 4.69 (d, J = 5.7 Hz, 2H), 3.54 (s, 2H), 3.24–3.16 (m, 4H), 2.89–2.83 (m, 1H), 2.81–2.65 (m, 2H), 2.13–2.07 (m, 1H), 1.59–1.56 (m, 2H), 1.47–1.41 (m, 2H), 1.39–1.33 (m, 2H), 1.31–1.26 (m, 2H). ^{13}C NMR (150 MHz, $CDCl_3$) δ 171.11, 170.87, 169.70, 168.56, 167.74, 167.27, 160.81, 151.72, 147.09, 139.12, 136.28, 135.83, 134.49, 132.60, 132.53, 129.54, 129.05, 128.77, 128.36, 127.82, 127.46 (q, J = 3.7 Hz), 127.07, 126.92, 125.71, 125.40 (q, J = 32.7 Hz), 124.26 (q, J = 271.6 Hz), 124.12, 122.80, 117.89, 116.91, 116.81, 111.61, 110.03, 49.02, 44.18, 43.83, 42.59, 39.68, 31.53, 29.49, 29.09, 26.61, 26.58, 22.93. LRMS (ESI) *m/z*: 834.2 $[M + H]^+$. HRMS (ESI): *m/z* calcd for $C_{46}H_{43}F_3N_5O_7^+$ $[M + H]^+$, 834.3114; found, 834.3107.

N-(3-(2-((8-((2-(2,6-dioxopiperidin-3-yl)-1,3-dioxoisoindolin-4-yl)amino)octyl)amino)-2-oxoethyl)benzyl)-5-(4-(trifluoromethyl) phenoxy)-2-naphthamide (**3**). Compound **3** was synthesized from **25** and **26c** using a similar procedure for the preparation of compound **1**. It was obtained as a white solid (6.3 mg, 35 % yield). ^{1}H NMR (600 MHz, Chloroform-*d*) δ 8.39 (d, J = 1.8 Hz, 1H), 8.20 (s, 1H), 8.14–8.08 (m, 1H), 7.85 (dd, J = 8.8, 1.8 Hz, 1H), 7.77 (d, J = 8.2 Hz, 1H), 7.61–7.55 (m, 2H), 7.53–7.43 (m, 2H), 7.36–7.28 (m, 3H), 7.19 (dt, J = 7.3, 1.7 Hz, 1H), 7.13 (dd, J = 7.6, 1.0 Hz, 1H), 7.09–7.03 (m, 3H), 6.85 (d, J = 8.6 Hz, 1H), 6.76 (t, J = 5.8 Hz, 1H), 6.21 (t, J = 5.6 Hz, 1H), 5.51–5.42 (m, 1H), 4.88 (dd, J = 12.4, 5.4 Hz, 1H), 4.70 (d, J = 5.7 Hz, 2H), 3.54 (s, 2H), 3.28–3.15 (m, 4H), 2.89–2.64 (m, 3H), 2.14–2.06 (m, 1H), 1.66–1.60 (m, 2H), 1.44–1.33 (m, 4H), 1.31–1.24 (m, 6H). ^{13}C NMR (150 MHz, $CDCl_3$) δ 171.28, 170.88, 169.67, 168.66, 167.78, 167.27, 160.83, 151.68, 147.12, 139.09, 136.23, 135.82, 134.48, 132.59, 132.53, 129.44, 129.05, 128.73, 128.34, 127.84, 127.44 (q, J = 3.7 Hz), 127.00, 126.89, 125.73, 125.35 (q, J = 32.7 Hz), 124.25 (q, J = 271.5 Hz), 124.18, 122.71, 117.85, 116.89, 116.79, 111.50, 109.95, 48.98, 44.15, 43.76, 42.63, 39.86, 31.51, 29.51, 29.09, 29.07, 29.05, 26.74, 26.69, 22.91. LRMS (ESI) *m/z*: 862.2 $[M + H]^+$. HRMS (ESI): *m/z* calcd for $C_{48}H_{47}F_3N_5O_7^+$ $[M + H]^+$, 862.3427; found, 862.3414.

N-(3-(2-((10-((2-(2,6-dioxopiperidin-3-yl)-1,3-dioxoisoindolin-4-yl)amino)decyl)amino)-2-oxoethyl)benzyl)-5-(4-(trifluoromethyl)phenoxy)-2-naphthamide (**4**). Compound **4** was synthesized from **25** and **26d** using a similar procedure for the preparation of compound **1**. It was obtained as a white solid (9.5 mg, 51 % yield). ^{1}H NMR (600 MHz, Chloroform-*d*) δ 8.39 (d, J = 1.8 Hz, 1H), 8.16 (s, 1H), 8.12 (d, J = 8.7 Hz, 1H), 7.85 (dd, J = 8.8, 1.8 Hz, 1H), 7.78 (d, J = 8.3 Hz, 1H), 7.58 (d, J = 8.7 Hz, 2H), 7.53–7.44 (m, 2H), 7.37–7.30 (m, 2H), 7.30–7.27 (m, 1H), 7.19 (dt, J = 7.3, 1.6 Hz, 1H), 7.14 (dd, J = 7.5, 1.0 Hz, 1H), 7.09–7.03 (m, 3H), 6.86 (d, J = 8.6 Hz, 1H), 6.73 (t, J = 5.8 Hz, 1H), 6.21 (t, J = 5.5 Hz, 1H), 5.49–5.38 (m, 1H), 4.89 (dd, J = 12.4, 5.4 Hz, 1H), 4.75–4.66 (m, 2H), 3.54 (s, 2H), 3.27–3.22 (m, 2H), 3.21–3.15 (m, 2H), 2.89–2.82 (m, 1H), 2.82–2.65 (m, 2H), 2.14–2.06 (m, 1H), 1.68–1.61 (m, 2H), 1.46–1.35 (m, 4H), 1.33–1.22 (m, 10H). ^{13}C NMR (150 MHz, $CDCl_3$) δ 171.16, 170.80, 169.66, 168.53, 167.80, 167.25, 160.84, 151.71, 147.17, 139.08, 136.24, 135.84, 134.50, 132.61, 132.54, 129.52, 129.09, 128.81, 128.37, 127.82, 127.45 (q, J = 3.7 Hz), 127.05, 126.94, 125.73, 125.37 (q, J = 32.7 Hz), 124.26 (q, J = 271.5 Hz), 124.14, 122.78, 117.87, 116.92, 116.79, 111.48, 109.94,

48.99, 44.19, 43.82, 42.72, 39.90, 31.54, 29.58, 29.39, 29.37, 29.26, 29.23, 29.21, 26.95, 26.87, 22.93. LRMS (ESI) *m/z*: 890.4 $[M + H]^+$. HRMS (ESI): *m/z* calcd for $C_{50}H_{51}F_3N_5O_7^+$ $[M + H]^+$, 890.3740; found, 890.3731.

N-(3-(2-((2-(2-((2-(2,6-dioxopiperidin-3-yl)-1,3-dioxoisoindolin-4-yl)amino)ethoxy)ethyl)amino)-2-oxoethyl)benzyl)-5-(4-(trifluoromethyl)phenoxy)-2-naphthamide (**5**). Compound **5** was synthesized from **25** and **27a** using a similar procedure for the preparation of compound **1**. It was obtained as a white solid (6.4 mg, 37 % yield). ^{1}H NMR (600 MHz, Chloroform-*d*) δ 8.42 (d, $J = 1.7$ Hz, 1H), 8.21 (s, 1H), 8.04 (d, $J = 8.8$ Hz, 1H), 7.87 (dd, $J = 8.8$, 1.8 Hz, 1H), 7.73 (d, $J = 8.3$ Hz, 1H), 7.61–7.54 (m, 2H), 7.49–7.42 (m, 2H), 7.30–7.26 (m, 2H), 7.26–7.23 (m, 1H), 7.23–7.20 (m, 1H), 7.13–7.08 (m, 2H), 7.08–7.03 (m, 3H), 6.81 (d, $J = 8.5$ Hz, 1H), 6.57 (t, $J = 5.2$ Hz, 1H), 6.45 (t, $J = 5.6$ Hz, 1H), 4.77 (dd, $J = 12.5$, 5.3 Hz, 1H), 4.64 (d, $J = 5.6$ Hz, 2H), 3.66 (t, $J = 5.1$ Hz, 2H), 3.61–3.53 (m, 4H), 3.52–3.45 (m, 2H), 3.39–3.33 (m, 2H), 2.71–2.60 (m, 2H), 2.58–2.48 (m, 1H), 2.06–1.94 (m, 1H). ^{13}C NMR (150 MHz, $CDCl_3$) δ 171.26, 171.18, 170.02, 168.74, 167.56, 167.18, 160.86, 151.60, 146.86, 138.92, 136.39, 136.05, 134.46, 132.51, 132.39, 129.19, 128.89, 128.47, 128.27, 127.94, 127.43 (q, $J = 3.8$ Hz), 126.84, 126.82, 125.80, 125.29 (q, $J = 33.0$ Hz), 124.31, 124.27 (q, $J = 271.6$ Hz), 122.49, 117.82, 116.95, 116.82, 112.05, 110.32, 70.01, 68.78, 49.04, 44.20, 43.28, 42.02, 39.51, 31.39, 22.81. LRMS (ESI) *m/z*: 822.4 $[M + H]^+$. HRMS (ESI): *m/z* calcd for $C_{44}H_{39}F_3N_5O_8^+$ $[M + H]^+$, 822.2750; found, 822.2741.

N-(3-(2-((2-(2-(2-((2-(2,6-dioxopiperidin-3-yl)-1,3-dioxoisoindolin-4-yl)amino)ethoxy)ethoxy)ethyl)amino)-2-oxoethyl)benzyl)-5-(4-(trifluoromethyl)phenoxy)-2-naphthamide (**6**). Compound **6** was synthesized from **25** and **27b** using a similar procedure for the preparation of compound **1**. It was obtained as a white solid (10.7 mg, 59 % yield). ^{1}H NMR (600 MHz, Chloroform-*d*) δ 8.52 (s, 1H), 8.41 (d, $J = 1.7$ Hz, 1H), 8.07 (d, $J = 8.7$ Hz, 1H), 7.87 (dd, $J = 8.8$, 1.7 Hz, 1H), 7.75 (d, $J = 8.3$ Hz, 1H), 7.58 (d, $J = 8.6$ Hz, 2H), 7.48 (t, $J = 7.9$ Hz, 1H), 7.43 (dd, $J = 8.5$, 7.1 Hz, 1H), 7.31–7.26 (m, 3H), 7.19 (dt, $J = 7.0$, 1.9 Hz, 1H), 7.12 (dd, $J = 7.6$, 1.0 Hz, 1H), 7.08–7.00 (m, 4H), 6.82 (d, $J = 8.5$ Hz, 1H), 6.47 (t, $J = 5.4$ Hz, 1H), 6.16 (t, $J = 5.6$ Hz, 1H), 4.77 (dd, $J = 12.2$, 5.4 Hz, 1H), 4.72–4.61 (m, 2H), 3.67 (t, $J = 5.2$ Hz, 2H), 3.63–3.50 (m, 8H), 3.46–3.36 (m, 4H), 2.78–2.72 (m, 1H), 2.70–2.55 (m, 2H), 2.06–1.98 (m, 1H). ^{13}C NMR (150 MHz, $CDCl_3$) δ 171.42, 171.14, 169.49, 168.85, 167.66, 167.25, 160.87, 151.67, 146.80, 138.97, 136.22, 135.85, 134.49, 132.62, 129.25, 129.11, 128.74, 128.31, 127.89, 127.45 (q, $J = 3.8$ Hz), 126.93, 126.89, 125.78, 125.33 (q, $J = 32.8$ Hz), 124.30, 124.27 (q, $J = 271.4$ Hz), 122.62, 117.86, 116.85, 116.78, 111.88, 110.45, 110.42, 70.88, 70.19, 69.92, 69.17, 48.93, 44.18, 43.54, 42.35, 39.69, 31.38, 22.93. LRMS (ESI) *m/z*: 866.2 $[M + H]^+$. HRMS (ESI): *m/z* calcd for $C_{46}H_{43}F_3N_5O_9^+$ $[M + H]^+$, 866.3013; found, 866.3004.

N-(3-(14-((2-(2,6-dioxopiperidin-3-yl)-1,3-dioxoisoindolin-4-yl)amino)-2-oxo-6,9,12-trioxa-3-azatetradecyl)benzyl)-5-(4-(trifluoromethyl)phenoxy)-2-naphthamide (**7**). Compound **7** was synthesized from **25** and **27c** using a similar procedure for the preparation of compound **1**. It was obtained as a white solid (10.3 mg, 54 % yield). ^{1}H NMR (600 MHz, Chloroform-*d*) δ 8.49–8.38 (m, 2H), 8.09 (d, $J = 8.7$ Hz, 1H), 7.87 (dd, $J = 8.8$, 1.8 Hz, 1H), 7.76 (d, $J = 8.3$ Hz, 1H), 7.61–7.55 (m, 2H), 7.48 (t, $J = 7.9$ Hz, 1H), 7.43 (dd, $J = 8.6$, 7.1 Hz, 1H), 7.33–7.27 (m, 3H), 7.19 (dt, $J = 6.6$, 1.9 Hz, 1H), 7.12 (dd, $J = 7.6$, 1.0 Hz, 1H), 7.08–7.02 (m, 3H), 7.00 (t, $J = 5.7$ Hz, 1H), 6.84 (d, $J = 8.5$ Hz, 1H), 6.46 (t, $J = 5.5$ Hz, 1H), 6.17 (t, $J = 5.7$ Hz, 1H), 4.88–4.82 (m, 1H), 4.72–4.64 (m, 2H), 3.68 (t, $J = 5.3$ Hz, 2H), 3.65–3.61 (m, 4H), 3.59–3.55 (m, 2H), 3.55–3.52 (m, 4H), 3.49 (t, $J = 5.2$ Hz, 2H), 3.43–3.36 (m, 4H), 2.83–2.77 (m, 1H), 2.75–2.62 (m, 2H), 2.09–2.03 (m, 1H). ^{13}C NMR (150 MHz, $CDCl_3$) δ 171.44, 171.19, 169.43, 168.78, 167.72, 167.21, 160.86, 151.66, 146.84, 139.00, 136.18, 135.84, 134.49, 132.60, 129.30, 129.10, 128.75, 128.30, 127.88, 127.44 (q, $J = 3.7$ Hz), 126.93, 125.77, 125.32 (q, $J = 32.7$ Hz), 124.33, 124.27 (q, $J = 271.4$ Hz), 122.61, 117.86, 116.84, 116.82, 111.83, 110.40, 70.90, 70.68, 70.58, 70.23, 69.78, 69.48, 48.97, 44.18, 43.57, 42.45, 39.50, 31.47, 22.89. LRMS (ESI) *m/z*: 910.4 $[M + H]^+$. HRMS (ESI): *m/z* calcd for $C_{48}H_{47}F_3N_5O_{10}^+$ $[M + H]^+$, 910.3275; found, 910.3266.

N-(3-(17-((2-(2,6-dioxopiperidin-3-yl)-1,3-dioxoisoindolin-4-yl)amino)-2-oxo-6,9,12,15-tetraoxa-3-azaheptadecyl)benzyl)-5-(4-(trifluoromethyl)phenoxy)-2-naphthamide (**8**). Compound **8** was synthesized from **25** and **27d** using a similar procedure for the preparation of compound **1**. It was obtained as a white solid (3.5 mg, 18 % yield). ^{1}H NMR (600 MHz, Chloroform-*d*) δ 8.60 (s, 1H), 8.42 (d, $J = 1.7$ Hz, 1H), 8.09 (d, $J = 8.7$ Hz, 1H), 7.89 (dd, $J = 8.8$, 1.7 Hz, 1H), 7.77 (d, $J = 8.3$ Hz, 1H), 7.61–7.55 (m, 2H), 7.48 (t, $J = 7.9$ Hz, 1H), 7.44 (dd, $J = 8.5$, 7.1 Hz, 1H), 7.33–7.27 (m, 3H), 7.20 (dt, $J = 7.0$, 1.9 Hz, 1H), 7.12 (dd, $J = 7.6$, 1.0 Hz, 1H), 7.08–7.03 (m, 3H), 7.01 (t, $J = 5.8$ Hz, 1H), 6.83 (d, $J = 8.5$ Hz, 1H), 6.50–6.42 (m, 2H), 4.83 (dd, $J = 12.3$, 5.4 Hz, 1H), 4.73–4.62 (m, 2H), 3.69–3.59 (m, 10H), 3.56–3.48 (m, 8H), 3.44–3.36 (m, 4H), 2.85–2.77 (m, 1H), 2.76–2.60 (m, 2H), 2.10–2.03 (m, 1H). ^{13}C NMR (150 MHz, $CDCl_3$) δ 171.49, 171.09, 169.39, 168.85, 167.75, 167.18, 160.87, 151.68, 146.88, 138.99, 136.19, 136.02, 134.51, 132.67, 132.62, 129.29, 129.04, 128.76, 128.31, 127.89, 127.45 (q, $J = 3.6$ Hz), 126.95, 126.91, 125.77, 125.34 (q, $J = 32.8$ Hz), 124.36, 124.31 (q, $J = 271.6$ Hz), 122.62, 117.87, 116.86, 116.84, 111.82, 110.40, 71.02, 70.77, 70.65, 70.64, 70.40, 70.30, 69.93, 69.41, 48.96, 44.23, 43.57, 42.42, 39.41, 31.48, 22.95. LRMS (ESI) *m/z*: 954.4 $[M + H]^+$. HRMS (ESI): *m/z* calcd for $C_{50}H_{51}F_3N_5O_{11}^+$ $[M + H]^+$, 954.3537; found, 954.3528.

Tert-butyl (3-((5-(4-(trifluoromethyl)phenoxy)-2-naphthamido)methyl)benzyl)carbamate (**29**). To a solution of compound **23** (300 mg, 0.90 mmol) in DMF (5 mL) was added DIEA (350.08 mg, 2.71 mmol), HATU (446.29 mg, 1.17 mmol), and tert-butyl (3-(aminomethyl)benzyl)carbamate **28** (234.69 mg, 0.99 mmol), successively. The resulting mixture was stirred at room temperature for 2 h. After completion of the reaction by checking the thin layer chromatography, the mixture was extracted with EtOAc. The combined organic layers were washed with brine and then concentrated. The residue was purified by flash column chromatography (0 %–40 % of EtOAc in hexanes) to afford compound **29** (490 mg, 98 % yield) as a white solid. ^{1}H NMR (600 MHz, Chloroform-*d*) δ 8.38 (d, $J = 1.8$ Hz, 1H), 8.12 (d, $J = 8.7$ Hz, 1H), 7.85 (dd, $J = 8.8$, 1.8 Hz, 1H), 7.80–7.75 (m, 1H), 7.61–7.55 (m, 2H), 7.50 (t, $J = 7.9$ Hz, 1H), 7.33 (t, $J = 7.7$ Hz, 1H), 7.30–7.27 (m, 2H), 7.23 (d, $J = 7.5$ Hz, 1H), 7.14 (dd, $J = 7.6$, 1.0 Hz, 1H), 7.09–7.04 (m, 2H), 6.60 (t, $J = 5.7$ Hz, 1H), 4.88 (s, 1H), 4.69 (d, $J = 5.6$ Hz, 2H), 4.32 (d, $J = 6.0$ Hz, 2H), 1.44 (s, 9H). LRMS (ESI) *m/z*: 551.3 $[M + H]^+$.

N-(3-(aminomethyl)benzyl)-5-(4-(trifluoromethyl)phenoxy)-2-naphthamide (**30**). A solution of compound **29** (450 mg, 0.82 mmol) in 4 M HCl in dioxane (8 mL) was stirred at room temperature for 2 h. After completion of the reaction by checking the thin layer chromatography, the mixture was filtered, and the concentration of the filtrate to afford compound **30** (360 mg, 90 % yield) as a white

solid. ^{1}H NMR (600 MHz, Methanol-d_4) δ 8.52 (d, J = 1.8 Hz, 1H), 8.11 (d, J = 8.8 Hz, 1H), 7.95 (dd, J = 8.8, 1.8 Hz, 1H), 7.90 (d, J = 8.3 Hz, 1H), 7.69–7.63 (m, 2H), 7.59 (t, J = 7.9 Hz, 1H), 7.51 (d, J = 1.9 Hz, 1H), 7.48 (dt, J = 7.7, 1.6 Hz, 1H), 7.45 (t, J = 7.5 Hz, 1H), 7.37 (dt, J = 7.4, 1.7 Hz, 1H), 7.24 (dd, J = 7.6, 1.0 Hz, 1H), 7.16–7.10 (m, 2H), 4.67 (s, 2H), 4.12 (s, 2H). LRMS (ESI) m/z: 451.0 $[M + H]^+$.

Tert-butyl 2-(1-(2-(2,6-dioxopiperidin-3-yl)-1,3-dioxoisoindolin-5-yl)piperidin-4-yl)acetate (**33**). To a solution of 2-(2,6-dioxopiperidin-3-yl)-5-fluoroisoindoline-1,3-dione **31** (100 mg, 0.362 mmol) in DMSO (2 mL) was added DIEA (93.58 mg, 0.724 mmol), and tert-butyl 2-(piperidin-4-yl)acetate **32** (79.36 mg, 0.398 mmol). The resulting mixture was stirred at 90 °C overnight. After completion of the reaction by checking the thin layer chromatography, the mixture was extracted with EtOAc. The combined organic layers were washed with brine and then concentrated. The residue was purified by flash column chromatography (0 %–40 % of EtOAc in hexanes) to afford compound **33** (140 mg, 85 % yield) as a yellow solid. ^{1}H NMR (600 MHz, Chloroform-d) δ 8.00 (s, 1H), 7.67 (d, J = 8.5 Hz, 1H), 7.27 (d, J = 2.5 Hz, 1H), 7.03 (dd, J = 8.6, 2.4 Hz, 1H), 4.93 (dd, J = 12.5, 5.4 Hz, 1H), 3.93 (dt, J = 13.6, 3.5 Hz, 2H), 3.00 (td, J = 12.8, 2.6 Hz, 2H), 2.92–2.86 (m, 1H), 2.84–2.78 (m, 1H), 2.77–2.69 (m, 1H), 2.19 (d, J = 7.1 Hz, 2H), 2.15–2.10 (m, 1H), 2.08–1.99 (m, 1H), 1.88–1.81 (m, 2H), 1.46 (s, 9H), 1.39–1.30 (m, 2H). LRMS (ESI) m/z: 456.1 $[M + H]^+$.

N-(3-((2-(1-(2-(2,6-dioxopiperidin-3-yl)-1,3-dioxoisoindolin-5-yl)piperidin-4-yl)acetamido)methyl)benzyl)-5-(4-(trifluoromethyl)phenoxy)-2-naphthamide (**9**). A solution of compound **33** (160 mg, 0.35 mmol) in 4 M HCl in dioxane (6 mL) was stirred at room temperature overnight. After completion of the reaction by checking the thin layer chromatography, the mixture was concentrated directly to afford the crude product (>99 % yield) as a white solid. To a solution of the above crude product (10 mg, 0.025 mmol) in DMF (0.5 mL) was added DIEA (16.18 mg, 0.125 mmol), HATU (12.38 mg, 0.032 mmol), and compound **30** (12.19 mg, 0.025 mmol), successively. The resulting mixture was stirred at room temperature overnight. After completion of the reaction by checking the thin layer chromatography, the mixture was extracted with EtOAc. The combined organic layers were washed with brine and then concentrated. The residue was purified by flash column chromatography (0 %–4 % of MeOH in EtOAc) to afford compound **9** (17.8 mg, 85 % yield) as a yellow solid. ^{1}H NMR (600 MHz, Chloroform-d) δ 8.41–8.31 (m, 2H), 8.09 (d, J = 8.8 Hz, 1H), 7.84 (dd, J = 8.8, 1.8 Hz, 1H), 7.73 (d, J = 8.3 Hz, 1H), 7.57 (d, J = 8.6 Hz, 3H), 7.47 (t, J = 7.9 Hz, 1H), 7.32–7.28 (m, 1H), 7.28–7.26 (m, 2H), 7.20–7.15 (m, 2H), 7.11 (dd, J = 7.6, 1.0 Hz, 1H), 7.04 (d, J = 8.6 Hz, 2H), 6.96 (t, J = 5.8 Hz, 1H), 6.91 (dd, J = 8.6, 2.4 Hz, 1H), 6.19 (t, J = 5.8 Hz, 1H), 4.88 (dd, J = 12.5, 5.4 Hz, 1H), 4.64 (d, J = 5.8 Hz, 2H), 4.41 (d, J = 5.7 Hz, 2H), 3.87–3.75 (m, 2H), 2.91–2.79 (m, 3H), 2.79–2.72 (m, 1H), 2.72–2.64 (m, 1H), 2.14–2.04 (m, 4H), 1.79–1.75 (m, 2H), 1.25–1.19 (m, 2H). ^{13}C NMR (150 MHz, $CDCl_3$) δ 171.55, 171.29, 168.70, 168.19, 167.39, 167.30, 160.76, 155.29, 151.70, 139.08, 138.96, 134.47, 134.45, 132.49, 129.30, 128.32, 127.82, 127.45 (q, J = 3.7 Hz), 127.22, 127.14, 127.10, 127.08, 125.67, 125.55, 125.39 (q, J = 32.7 Hz), 124.24 (q, J = 271.7 Hz), 124.13, 122.77, 118.57, 117.89, 117.86, 116.89, 108.63, 49.24, 48.09, 48.06, 44.13, 43.55, 43.32, 33.28, 31.56, 31.31, 31.28, 22.82. LRMS (ESI) m/z: 832.4 $[M + H]^+$. HRMS (ESI): m/z calcd for $C_{46}H_{41}F_3N_5O_7^+$ $[M + H]^+$, 832.2958; found, 832.2947.

3-(1-oxo-5-(piperazin-1-yl)isoindolin-2-yl)piperidine-2,6-dione hydrochloride (**35**). Compound **35** was synthesized from **34** using a similar procedure for the preparation of compound **30**. It was obtained as a white solid. ^{1}H NMR (600 MHz, DMSO-d_6) δ 10.95 (s, 1H), 9.57 (s, 2H), 7.57 (d, J = 8.5 Hz, 1H), 7.15 (d, J = 2.2 Hz, 1H), 7.12 (dd, J = 8.5, 2.2 Hz, 1H), 5.05 (dd, J = 13.3, 5.1 Hz, 1H), 4.35 (d, J = 16.9 Hz, 1H), 4.23 (d, J = 17.0 Hz, 1H), 3.54 (d, J = 5.3 Hz, 4H), 3.23–3.15 (m, 4H), 2.94–2.84 (m, 1H), 2.63–2.54 (m, 1H), 2.42–2.32 (m, 1H), 1.99–1.93 (m, 1H). LRMS (ESI) m/z: 329.1 $[M + H]^+$.

Tert-butyl 2-(4-(hydroxymethyl)piperidin-1-yl)acetate (**38**). A solution of piperidin-4-ylmethanol **36** (1.48 g, 12.82 mmol) and tert-butyl 2-bromoacetate **37** (1 g, 5.13 mmol) in THF (10 mL) was stirred at room temperature overnight. After completion of the reaction by checking the thin layer chromatography, the mixture was extracted with EtOAc. The combined organic layers were washed with brine and then concentrated. The residue was purified by flash column chromatography (0 %–20 % of MeOH in DCM) to afford compound **38** (2.15 g, 68 % yield) as a colorless oil. ^{1}H NMR (600 MHz, Chloroform-d) δ 3.48 (d, J = 6.5 Hz, 2H), 3.09 (s, 2H), 2.98–2.92 (m, 2H), 2.15 (td, J = 11.6, 2.6 Hz, 2H), 1.75–1.67 (m, 2H), 1.45 (s, 10H), 1.39–1.29 (m, 2H). LRMS (ESI) m/z: 230.0 $[M + H]^+$

Tert-butyl 2-(4-((4-(2-(2,6-dioxopiperidin-3-yl)-1-oxoisoindolin-5-yl)piperazin-1-yl)methyl)piperidin-1-yl)acetate (**39**). To a solution of oxalyl chloride (387 mg, 3.05 mmol) in DCM (8 mL) was added DMSO (340 mg, 4.36 mmol) dropwise at −78 °C under N_2 atmosphere. The mixture was stirred at −78 °C for 15 min, then a solution of compound **38** (500 mg, 2.18 mmol) in DCM (2 mL) was added dropwise. The resulting mixture was stirred at −78 °C for another 30 min. TEA (1.1 g, 10.90 mmol) was added and the mixture was warmed to room temperature. The reaction mixture was stirred for 2 h. After completion of the reaction by checking the thin layer chromatography, the mixture was quenched by adding saturated aqueous NH_4Cl and extracted with EtOAc. The combined organic layers were washed with brine, then dried over Na_2SO_4, filtered, and concentrated to afford crude aldehyde product (478 mg, 96 % yield) as a light brown oil. To a solution of compound **35** (80 mg, 0.219 mmol) in DCM (2 mL) and MeOH (2 mL) was added KOAc (64.56 mg, 0.657 mmol), the above crude aldehyde product (64.8 mg, 0.285 mmol), and $NaBH_3CN$ (41.34 mg, 0.657 mmol), successively. The resulting mixture was stirred at room temperature overnight. After completion of the reaction by checking the thin layer chromatography, the mixture was extracted with EtOAc. The combined organic layers were washed with brine and then concentrated. The residue was purified by flash column chromatography (0 %–20 % of MeOH in DCM) to afford compound **39** (100 mg, 85 % yield) as a yellow oil. ^{1}H NMR (600 MHz, Methanol-d_4) δ 7.63 (d, J = 8.6 Hz, 1H), 7.11–7.04 (m, 2H), 5.09 (dd, J = 13.3, 5.2 Hz, 1H), 4.44–4.34 (m, 2H), 3.37–3.33 (m, 4H), 3.11 (s, 2H), 2.96 (dt, J = 11.9, 3.4 Hz, 2H), 2.93–2.85 (m, 1H), 2.81–2.74 (m, 1H), 2.58 (t, J = 5.1 Hz, 4H), 2.50–2.41 (m, 1H), 2.27 (d, J = 7.1 Hz, 2H), 2.20–2.12 (m, 3H), 1.82–1.75 (m, 2H), 1.66–1.57 (m, 1H), 1.48 (s, 9H), 1.35–1.27 (m, 2H). LRMS (ESI) m/z: 540.2 $[M + H]^+$.

N-(3-((2-(4-((4-(2-(2,6-dioxopiperidin-3-yl)-1-oxoisoindolin-5-yl)piperazin-1-yl)methyl)piperidin-1-yl)acetamido)methyl) benzyl)-5-(4-(trifluoromethyl)phenoxy)-2-naphthamide (**10**). Compound **10** was synthesized from **30** and **39** using a similar procedure for the preparation of compound **9**. It was obtained as a white solid (10 mg, 44 % yield). ^{1}H NMR (600 MHz, Chloroform-d) δ

8.40 (d, $J = 1.7$ Hz, 1H), 8.20–8.06 (m, 2H), 7.86 (dd, $J = 8.8$, 1.8 Hz, 1H), 7.78 (d, $J = 8.3$ Hz, 1H), 7.71 (d, $J = 8.6$ Hz, 1H), 7.61 (t, $J = 6.2$ Hz, 1H), 7.59–7.56 (m, 2H), 7.50 (t, $J = 7.9$ Hz, 1H), 7.34 (t, $J = 7.5$ Hz, 1H), 7.32–7.28 (m, 2H), 7.21 (dt, $J = 7.5$, 1.6 Hz, 1H), 7.13 (dd, $J = 7.6$, 1.0 Hz, 1H), 7.08–7.04 (m, 2H), 6.96 (dd, $J = 8.6$, 2.2 Hz, 1H), 6.85 (d, $J = 2.1$ Hz, 1H), 6.74 (t, $J = 5.8$ Hz, 1H), 5.17 (dd, $J = 13.3$, 5.1 Hz, 1H), 4.70 (d, $J = 5.7$ Hz, 2H), 4.48 (d, $J = 6.1$ Hz, 2H), 4.39 (d, $J = 15.6$ Hz, 1H), 4.24 (d, $J = 15.6$ Hz, 1H), 3.28 (t, $J = 5.1$ Hz, 4H), 3.03 (s, 2H), 2.92–2.76 (m, 4H), 2.51 (t, $J = 5.1$ Hz, 4H), 2.34–2.26 (m, 1H), 2.22–2.10 (m, 6H), 1.75–1.71 (m, 2H), 1.21–1.14 (m, 2H). ^{13}C NMR (150 MHz, $CDCl_3$) δ 171.28, 170.98, 169.91, 169.71, 169.70, 167.21, 160.83, 154.60, 151.72, 143.77, 139.46, 138.79, 134.50, 132.60, 129.35, 128.37, 127.77, 127.46 (q, $J = 3.7$ Hz), 127.09, 127.07, 126.85, 125.73, 125.39 (q, $J = 32.9$ Hz), 125.14, 124.25 (q, $J = 271.5$ Hz), 124.16, 122.81, 121.82, 117.88, 116.92, 115.53, 108.29, 64.53, 62.11, 54.39, 53.44, 51.84, 48.39, 47.03, 44.27, 42.83, 32.74, 31.74, 31.15, 23.61. LRMS (ESI) *m/z*: 916.4 $[M + H]^+$. HRMS (ESI): *m/z* calcd for $C_{51}H_{53}F_3N_7O_6^+$ $[M + H]^+$, 916.4009; found, 916.4001.

N-(3-formylbenzyl)-5-(4-(trifluoromethyl)phenoxy)-2-naphthamide (**41**). A solution of tert-butyl tert-butyl (3-formylbenzyl) carbamate **40** (156 mg, 0.66 mmol) in 4 M HCl in dioxane (10 mL) was stirred at room temperature for 1 h. After completion of the reaction by checking the thin layer chromatography, the mixture was concentrated to afford the crude product, which was used directly without purification. To a solution of compound **23** (200 mg, 0.60 mmol) in DMF (5 mL) was added DIEA (388.97 mg, 3.01 mmol), HATU (297.53 mg, 0.78 mmol), and the above crude product, successively. The resulting mixture was stirred at room temperature for 2 h. After completion of the reaction by checking the thin layer chromatography, the mixture was extracted with EtOAc. The combined organic layers were washed with brine and then concentrated. The residue was purified by flash column chromatography (0 %–30 % of EtOAc in hexanes) to afford compound **41** (241 mg, 89 % yield for two steps) as a white solid. ^{1}H NMR (600 MHz, Chloroform-*d*) δ 10.02 (s, 1H), 8.40 (d, $J = 1.7$ Hz, 1H), 8.14 (d, $J = 8.7$ Hz, 1H), 7.90 (t, $J = 1.8$ Hz, 1H), 7.85 (dd, $J = 8.8$, 1.8 Hz, 1H), 7.82 (dt, $J = 7.6$, 1.4 Hz, 1H), 7.78 (d, $J = 8.2$ Hz, 1H), 7.69 (dt, $J = 7.7$, 1.4 Hz, 1H), 7.59 (d, $J = 8.7$ Hz, 2H), 7.54 (t, $J = 7.6$ Hz, 1H), 7.51 (t, $J = 7.9$ Hz, 1H), 7.14 (dd, $J = 7.6$, 1.0 Hz, 1H), 7.10–7.03 (m, 2H), 6.73 (t, $J = 6.0$ Hz, 1H), 4.80 (d, $J = 5.9$ Hz, 2H). LRMS (ESI) *m/z*: 450.1 $[M + H]^+$.

Tert-butyl 4-((4-(2-(2,6-dioxopiperidin-3-yl)-1-oxoisoindolin-5-yl)piperazin-1-yl)methyl)piperidine-1-carboxylate (**43**). To a solution of compound (**35**) (200 mg, 0.548 mmol) in DMSO (2 mL) and DCM (2 mL) was added DIEA (212.56 mg, 1.64 mmol), tert-butyl 4-formylpiperidine-1-carboxylate **42** (163.69 mg, 0.767 mmol), and $NaBH(OAc)_3$ (348.56 mg, 1.64 mmol). The mixture was stirred at room temperature overnight. After completion of the reaction by checking the thin layer chromatography, the mixture was quenched with saturated aqueous $NaHCO_3$ solution. The mixture was extracted with EtOAc. The combined organic layers were washed with brine and then concentrated. The residue was purified by flash column chromatography (0 %–100 % of EtOAc in hexanes) to afford compound **43** (130 mg, 45 % yield) as a white solid. ^{1}H NMR (600 MHz, Chloroform-*d*) δ 8.08 (s, 1H), 7.73 (d, $J = 8.6$ Hz, 1H), 6.98 (dd, $J = 8.6$, 2.2 Hz, 1H), 6.87 (d, $J = 2.2$ Hz, 1H), 5.20 (dd, $J = 13.3$, 5.1 Hz, 1H), 4.40 (d, $J = 15.6$ Hz, 1H), 4.25 (d, $J = 15.6$ Hz, 1H), 4.21–3.95 (m, 2H), 3.37–3.25 (m, 4H), 2.94–2.78 (m, 2H), 2.70 (s, 2H), 2.60–2.52 (m, 4H), 2.36–2.27 (m, 1H), 2.25–2.16 (m, 3H), 1.75 (d, $J = 13.2$ Hz, 2H), 1.72–1.62 (m, 1H), 1.46 (s, 9H), 1.15–1.04 (m, 2H). LRMS (ESI) *m/z*: 526.2 $[M + H]^+$.

N-(3-((4-((4-(2-(2,6-dioxopiperidin-3-yl)-1-oxoisoindolin-5-yl)piperazin-1-yl)methyl)piperidin-1-yl)methyl)benzyl)-5-(4-(trifluoromethyl)phenoxy)-2-naphthamide (**11**). A solution of compound **43** (100 mg, 0.19 mmol) in DCM (2 mL) and 4 M HCl in dioxane (4 mL) was stirred at room temperature for 1 h. After completion of the reaction by checking the thin layer chromatography, the mixture was concentrated directly to afford the crude product (>99 % yield) as a white solid. To a solution of the above crude product (11.82 mg, 0.025 mmol) in MeOH (1 mL) was added KOAc (6.55 mg, 0.066 mmol), AcOH (0.1 mL), compound **41** (10 mg, 0.022 mmol), and $NaBH_3CN$ (4.19 mg, 0.066 mmol), successively. The resulting mixture was stirred at room temperature overnight. After completion of the reaction by checking the thin layer chromatography, the mixture was extracted with EtOAc. The combined organic layers were washed with brine and then concentrated. The residue was purified by flash column chromatography (0 %–10 % of MeOH in DCM) to afford compound **11** (11.5 mg, 57 % yield) as a white solid. ^{1}H NMR (600 MHz, Chloroform-*d*) δ 8.51–8.20 (m, 2H), 8.11 (d, $J = 8.8$ Hz, 1H), 7.87 (dd, $J = 8.8$, 1.8 Hz, 1H), 7.78 (d, $J = 8.3$ Hz, 1H), 7.70 (d, $J = 8.6$ Hz, 1H), 7.58 (d, $J = 8.6$ Hz, 2H), 7.49 (t, $J = 7.9$ Hz, 1H), 7.42 (s, 1H), 7.34–7.29 (m, 2H), 7.27–7.26 (m, 1H), 7.13 (dd, $J = 7.6$, 1.0 Hz, 1H), 7.06 (d, $J = 8.5$ Hz, 2H), 6.96 (dd, $J = 8.6$, 2.2 Hz, 1H), 6.85 (d, $J = 2.1$ Hz, 1H), 6.78 (s, 1H), 5.16 (dd, $J = 13.3$, 5.1 Hz, 1H), 4.71 (d, $J = 5.6$ Hz, 2H), 4.38 (d, $J = 15.6$ Hz, 1H), 4.23 (d, $J = 15.6$ Hz, 1H), 3.56 (s, 2H), 3.32–3.23 (m, 4H), 2.96 (d, $J = 11.1$ Hz, 2H), 2.90–2.84 (m, 1H), 2.82–2.75 (m, 1H), 2.53 (t, $J = 5.0$ Hz, 4H), 2.34–2.26 (m, 1H), 2.22 (d, $J = 7.1$ Hz, 2H), 2.18–2.14 (m, 1H), 2.04 (t, $J = 11.5$ Hz, 2H), 1.80–1.70 (m, 2H), 1.58–1.50 (m, 1H), 1.38–1.28 (m, 2H). ^{13}C NMR (150 MHz, $CDCl_3$) δ 171.40, 169.99, 169.70, 167.21, 160.85, 154.61, 151.67, 143.77, 138.36, 134.51, 132.72, 129.11, 128.87, 128.84, 128.33, 127.82, 127.43 (q, $J = 3.7$ Hz), 127.07, 126.97, 125.75, 125.32 (q, $J = 32.7$ Hz), 125.09, 124.25 (q, $J = 271.4$ Hz), 124.24, 122.71, 121.76, 117.83, 116.88, 115.48, 108.26, 64.59, 63.14, 53.70, 53.46, 51.84, 48.39, 47.04, 44.34, 33.19, 31.73, 30.59, 23.59. LRMS (ESI) *m/z*: 859.4 $[M + H]^+$. HRMS (ESI): *m/z* calcd for $C_{49}H_{50}F_3N_6O_5^+$ $[M + H]^+$, 859.3795; found, 859.3782.

N-(3-((4-(2-(2,6-dioxopiperidin-3-yl)-1-oxoisoindolin-5-yl)piperazin-1-yl)methyl)benzyl)-5-(4-(trifluoromethyl)phenoxy)-2-naphthamide (**12**). Compound **12** was synthesized from **41** and **35** using a similar procedure for the preparation of compound **11**. It was obtained as a white solid (7.3 mg, 43 % yield). ^{1}H NMR (600 MHz, Chloroform-*d*) δ 8.40 (d, $J = 1.7$ Hz, 1H), 8.32 (s, 1H), 8.11 (d, $J = 8.8$ Hz, 1H), 7.86 (dd, $J = 8.8$, 1.8 Hz, 1H), 7.75 (d, $J = 8.3$ Hz, 1H), 7.68 (d, $J = 8.6$ Hz, 1H), 7.61–7.54 (m, 2H), 7.48 (t, $J = 7.9$ Hz, 1H), 7.40–7.37 (m, 1H), 7.36–7.27 (m, 3H), 7.13 (dd, $J = 7.6$, 1.0 Hz, 1H), 7.05 (d, $J = 8.6$ Hz, 2H), 6.93 (dd, $J = 8.6$, 2.2 Hz, 1H), 6.83 (d, $J = 2.1$ Hz, 1H), 6.77 (t, $J = 5.8$ Hz, 1H), 5.15 (dd, $J = 13.3$, 5.1 Hz, 1H), 4.72 (d, $J = 5.7$ Hz, 2H), 4.37 (d, $J = 15.7$ Hz, 1H), 4.22 (d, $J = 15.7$ Hz, 1H), 3.57 (s, 2H), 3.29 (t, $J = 5.0$ Hz, 4H), 2.90–2.82 (m, 1H), 2.82–2.73 (m, 1H), 2.61 (t, $J = 5.0$ Hz, 4H), 2.34–2.24 (m, 1H), 2.18–2.12 (m, 1H). ^{13}C NMR (150 MHz, $CDCl_3$) δ 171.44, 170.00, 169.70, 167.23, 160.80, 154.54, 151.70, 143.77, 138.49, 134.48, 132.69, 128.96, 128.82, 128.67, 128.32, 127.78, 127.44 (q, $J = 3.7$ Hz), 127.05, 127.00, 125.66, 125.36 (q, $J = 32.8$ Hz), 125.09, 124.24 (q, $J = 271.4$ Hz), 124.14, 122.76, 121.85, 117.86, 116.88, 115.55, 108.36, 62.85, 52.87, 51.85, 48.34, 47.06, 44.31,

31.71, 23.56. LRMS (ESI) *m/z*: 762.3 $[M + H]^+$. HRMS (ESI): *m/z* calcd for $C_{43}H_{39}F_3N_5O_5^+$ $[M + H]^+$, 762.2903; found, 762.2892.

(S)-N-((S)-1-(6-bromopyridin-2-yl)ethyl)-2-methylpropane-2-sulfinamide (**46a**). To a solution of 1-(6-bromopyridin-2-yl)ethan-1-one **44** (4 g, 20.00 mmol) in THF (40 mL) was added $Ti(OEt)_4$ (9.12 g, 39.99 mmol) and (S)-2-methylpropane-2-sulfinamide **45a** (4.85 g, 39.99 mmol). The reaction mixture was heated to reflux overnight, whereupon it was allowed to cool to room temperature and stirred for 30 min. The reaction was cooled to −30 °C and $NaBH_4$ (1.51 g, 39.99 mmol) was added. The reaction mixture was stirred at 0–5 °C for 2 h and then quenched by drop-wise addition of water. The mixture was filtered through Celite, and the solids were washed with EtOAc. The organic layer was washed with brine, dried over sodium sulfate, and concentrated under reduced pressure. The residue was purified by flash column chromatography (0 %–70 % of EtOAc in hexanes) to afford compound **46a** (5.55 g, 91 % yield) as a brown solid. ^{1}H NMR (600 MHz, Chloroform-*d*) δ 7.51 (t, $J = 7.7$ Hz, 1H), 7.36 (dd, $J = 7.9$, 0.8 Hz, 1H), 7.28 (dd, $J = 7.6$, 0.9 Hz, 1H), 4.58–4.52 (m, 1H), 4.49 (d, $J = 6.3$ Hz, 1H), 1.51 (d, $J = 6.7$ Hz, 3H), 1.25 (s, 9H). LRMS (ESI) *m/z*: 305.0 $[M + H]^+$.

*Tert-butyl (S)-(1-(6-bromopyridin-*2-yl*)ethyl)carbamate* (**47a**). To a solution of compound **46a** (2.40 g, 7.86 mmol) in MeOH (12 mL) was added 4 M HCl in dioxane (12 mL). The mixture was stirred at room temperature for 1 h. After completion of the reaction by checking the thin layer chromatography, the mixture was concentrated to afford the crude product, which was used directly without purification. To a solution of the above crude product in DCM (30 mL) was added DIEA (3.05 g, 23.57 mmol) and di-tert-butyl decarbonate (2.57 g, 11.79 mmol). The mixture was stirred at room temperature for 1 h. After completion of the reaction by checking the thin layer chromatography, the mixture was extracted with DCM. The combined organic layers were washed with brine and then concentrated. The residue was purified by flash column chromatography (0 %–20 % of EtOAc in hexanes) to afford compound **47a** (2.22 g, 94 % yield) as a white solid. ^{1}H NMR (600 MHz, Chloroform-*d*) δ 7.49 (t, $J = 7.7$ Hz, 1H), 7.35 (d, $J = 7.7$ Hz, 1H), 7.20 (d, $J = 7.5$ Hz, 1H), 5.45 (d, $J = 7.5$ Hz, 1H), 4.81 (t, $J = 7.3$ Hz, 1H), 1.44 (d, $J = 6.8$ Hz, 12H). LRMS (ESI) *m/z*: 201.0 $[M + H]^+$.

Tert-butyl (S)-(1-(6-cyanopyridin-2-yl)ethyl)carbamate (**48a**). To a solution of compound **47a** (1.5 g, 4.98 mmol) in DMF (20 mL) was added $Zn(CN)_2$ (0.88 g, 7.47 mmol) and $Pd(PPh_3)_4$ (0.57 g, 0.49 mmol). The reaction mixture was stirred for 12 h at 100 °C and then cooled to room temperature. The mixture was filtered through a plug of celite and concentrated. The residue was extracted with EtOAc. The combined organic layers were washed with brine and then concentrated. The residue was purified by flash column chromatography (0 %–25 % of EtOAc in hexanes) to afford compound **48a** (1.10 g, 89 % yield) as a white solid. ^{1}H NMR (600 MHz, Chloroform-*d*) δ 7.79 (t, $J = 7.8$ Hz, 1H), 7.58 (dd, $J = 7.7$, 1.0 Hz, 1H), 7.48 (d, $J = 8.0$ Hz, 1H), 5.57–5.39 (m, 1H), 4.97–4.83 (m, 1H), 1.48–1.41 (m, 12H). LRMS (ESI) *m/z*: 248.0 $[M + H]^+$.

Tert-butyl (S)-(1-(6-formylpyridin-2-yl)ethyl)carbamate (**49a**). To a solution of compound **48a** (1.05 g, 4.25 mmol) in DCM (20 mL) was added DIBAL-H solution (5.31 mL, 6.37 mmol, 1.2 M in toluene) by dropwise at −78 °C under N_2 atmosphere. The reaction mixture was stirred at −78 °C under N_2 atmosphere for 2 h. After completion of the reaction by checking the thin layer chromatography, the mixture was quenched by adding water and extracted with EtOAc. The combined organic layers were washed with brine and then concentrated. The residue was purified by flash column chromatography (0 %–25 % of EtOAc in hexanes) to afford compound **49a** (260 mg, 25 % yield) as a light yellow solid. ^{1}H NMR (600 MHz, Chloroform-*d*) δ 10.07 (s, 1H), 7.87–7.80 (m, 2H), 7.48 (dd, $J =$ 6.6, 2.2 Hz, 1H), 5.72–5.57 (m, 1H), 5.02–4.88 (m, 1H), 1.50 (d, $J = 6.9$ Hz, 3H), 1.45 (s, 9H). LRMS (ESI) *m/z*: 251.0 $[M + H]^+$.

(S)-N-(1-(6-formylpyridin-2-yl)ethyl)-5-(4-(trifluoromethyl)phenoxy)-2-naphthamide (**50a**). A solution of tert-butyl (S)-(1-(6-formylpyridin-2-yl)ethyl)carbamate (150.66 mg, 0.60 mmol) in DCM (1 mL) and 4 M HCl in dioxane (2 mL) was stirred at room temperature for 1 h. After completion of the reaction by checking the thin layer chromatography, the mixture was concentrated to give the crude product, which was used directly without purification. To a solution of compound **23** (200 mg, 0.60 mmol) in DMF (5 mL) was added DIEA (388.97 mg, 3.01 mmol), HATU (297.53 mg, 0.78 mmol), and the above crude product, successively. The resulting mixture was stirred at room temperature for 2 h. After completion of the reaction by checking the thin layer chromatography, the mixture was extracted with EtOAc. The combined organic layers were washed with brine and then concentrated. The residue was purified by flash column chromatography (0 %–30 % of EtOAc in hexanes) to afford compound **50a** (210 mg, 75 % yield) as a white solid. ^{1}H NMR (600 MHz, Chloroform-*d*) δ 10.12 (s, 1H), 8.45 (d, $J = 1.7$ Hz, 1H), 8.15 (d, $J = 8.7$ Hz, 1H), 7.93–7.89 (m, 3H), 7.82 (d, $J = 8.2$ Hz, 1H), 7.78 (d, $J = 7.3$ Hz, 1H), 7.61–7.55 (m, 3H), 7.52 (t, $J = 7.9$ Hz, 1H), 7.15 (dd, $J = 7.6$, 1.0 Hz, 1H), 7.07 (d, $J = 8.7$ Hz, 2H), 5.60–5.46 (m, 1H), 1.68 (d, $J = 6.8$ Hz, 3H). LRMS (ESI) *m/z*: 465.2 $[M + H]^+$.

(R)-N-(1-(6-formylpyridin-2-yl)ethyl)-5-(4-(trifluoromethyl)phenoxy)-2-naphthamide (**50b**). Compound **50b** was synthesized from **44** and **45b** using a similar procedure for the preparation of compound **50a**. It was obtained as a white solid. ^{1}H NMR (600 MHz, Chloroform-*d*) δ 10.12 (s, 1H), 8.45 (d, $J = 1.7$ Hz, 1H), 8.16 (dt, $J = 8.8$, 0.8 Hz, 1H), 7.93–7.89 (m, 3H), 7.85–7.80 (m, 1H), 7.77 (d, $J = 7.4$ Hz, 1H), 7.62–7.56 (m, 3H), 7.52 (dd, $J = 8.3$, 7.5 Hz, 1H), 7.15 (dd, $J = 7.6$, 1.0 Hz, 1H), 7.10–7.05 (m, 2H), 5.57–5.50 (m, 1H), 1.68 (d, $J = 6.9$ Hz, 3H). LRMS (ESI) *m/z*: 465.0 $[M + H]^+$.

N-((1S)-1-(6-((4-(2-(2,6-dioxopiperidin-3-yl)-1-oxoisoindolin-5-yl)piperazin-1-yl)methyl)pyridin-2-yl)ethyl)-5-(4-(trifluoromethyl)phenoxy)-2-naphthamide (**13**). To a solution of compound **35** (5.50 mg, 0.015 mmol) in MeOH (1 mL) was added KOAc (4.44 mg, 0.045 mmol), AcOH (0.1 mL), compound **50a** (10 mg, 0.022 mmol), and $NaBH_3CN$ (4.19 mg, 0.66 mmol), successively. The resulting mixture was stirred at room temperature overnight. After completion of the reaction by checking the thin layer chromatography, the mixture was extracted with EtOAc. The combined organic layers were washed with brine and then concentrated. The residue was purified by flash column chromatography (0 %–10 % of MeOH in DCM) to afford compound **13** (4.3 mg, 37 % yield) as a white solid. ^{1}H NMR (600 MHz, Chloroform-*d*) δ 8.52–8.44 (m, 1H), 8.37 (d, $J = 10.2$ Hz, 1H), 8.16–8.05 (m, 2H), 7.93 (dd, $J = 8.7$, 1.7 Hz, 1H), 7.79 (dd, $J = 8.3$, 1.4 Hz, 1H), 7.69 (t, $J = 7.7$ Hz, 2H), 7.57 (d, $J = 8.5$ Hz, 2H), 7.47 (td, $J = 8.0$, 1.2 Hz, 1H), 7.38 (d, $J =$ 7.6 Hz, 1H), 7.23 (d, $J = 7.7$ Hz, 1H), 7.15–7.10 (m, 1H), 7.05 (d, $J = 8.5$ Hz, 2H), 6.91 (dt, $J = 8.8$, 2.7 Hz, 1H), 6.82 (t, $J = 2.5$ Hz, 1H), 5.45–5.34 (m, 1H), 5.23–5.13 (m, 1H), 4.37 (d, $J = 15.6$ Hz, 1H), 4.21 (d, $J = 15.6$ Hz, 1H), 3.87–3.71 (m, 2H), 3.31 (t, $J = 5.0$ Hz, 4H), 2.92–2.64 (m, 6H), 2.33–2.24 (m, 1H), 2.19–2.13 (m, 1H), 1.62 (d, $J = 6.8$ Hz, 3H). ^{13}C NMR (150 MHz, $CDCl_3$) δ 171.46, 170.02, 170.01, 169.64, 166.29, 160.87, 160.42, 157.62, 154.48, 151.64, 143.76, 137.65, 134.54, 133.11, 128.27, 127.85, 127.43 (q, $J = 3.8$

Hz), 126.94, 126.92, 125.76, 125.27 (q, J = 33.3 Hz), 125.12, 124.26, 124.25 (q, J = 272.0 Hz), 122.60, 122.01, 121.84, 120.10, 117.80, 116.86, 116.83, 115.58, 108.43, 64.27, 53.04, 51.84, 50.20, 48.42, 47.02, 31.72, 23.58, 23.14. LRMS (ESI) *m/z*: 777.3 $[M + H]^+$. HRMS (ESI): *m/z* calcd for $C_{43}H_{40}F_3N_6O_5^+$ $[M + H]^+$, 777.3012; found, 777.3000.

Tert-butyl 4-(4-((2,6-dioxopiperidin-3-yl)amino)-2-fluorophenyl)piperazine-1-carboxylate (**53**). A mixture of compound **51** (295 mg, 1.0 mmol), compound **52** (288 mg, 1.5 mmol), and DIEA (695 μL, 4.0 mmol) in DMSO (6 mL) was stirred at 70 °C overnight. The resulting mixture was cooled to room temperature and diluted with EtOAc, then washed with water and sat. aq. NH_4Cl. The organic layers were dried over Na_2SO_4, filtered, and concentrated. The residue was purified by flash column chromatography (20 %–80 % of EtOAc in hexanes) to afford **53** (290 mg, 71 % yield) as a light-green solid. ^{1}H NMR (600 MHz, Chloroform-*d*) δ 8.00 (s, 1H), 6.87 (t, J = 8.9 Hz, 1H), 6.49–6.39 (m, 2H), 4.64 (d, J = 3.8 Hz, 1H), 4.03 (dt, J = 12.5, 4.4 Hz, 1H), 3.60 (t, J = 5.0 Hz, 4H), 3.00–2.86 (m, 5H), 2.77 (m, 1H), 2.58–2.51 (m, 1H), 1.99–1.87 (m, 1H), 1.50 (s, 9H). LRMS (ESI) *m/z*: 407.1 $[M + H]^+$.

N-((1S)-1-(6-((4-(4-((2,6-dioxopiperidin-3-yl)amino)-2-fluorophenyl)piperazin-1-yl)methyl)pyridin-2-yl)ethyl)-5-(4-(trifluoromethyl)phenoxy)-2-naphthamide (**14**). Compound **14** was synthesized from **53** and **50a** using a similar procedure for the preparation of compound **11**. It was obtained as a colorless oil (3.97 mg, 31 % yield). ^{1}H NMR (600 MHz, Chloroform-*d*) δ 8.52–8.44 (m, 1H), 8.34 (d, J = 4.4 Hz, 1H), 8.21–8.10 (m, 2H), 7.93 (dd, J = 8.8, 1.7 Hz, 1H), 7.81 (d, J = 8.3 Hz, 1H), 7.68 (t, J = 7.7 Hz, 1H), 7.61–7.54 (m, 2H), 7.49 (t, J = 7.9 Hz, 1H), 7.41–7.35 (m, 1H), 7.21 (d, J = 7.6 Hz, 1H), 7.13 (dd, J = 7.6, 1.0 Hz, 1H), 7.06 (d, J = 8.5 Hz, 2H), 6.82 (t, J = 9.0 Hz, 1H), 6.44–6.33 (m, 2H), 5.44–5.33 (m, 1H), 4.66–4.54 (m, 1H), 4.02–3.92 (m, 1H), 3.80 (s, 2H), 3.11–2.95 (m, 4H), 2.90–2.82 (m, 1H), 2.80–2.65 (m, 5H), 2.54–2.44 (m, 1H), 1.93–1.82 (m, 1H), 1.62 (d, J = 6.7 Hz, 3H). ^{13}C NMR (150 MHz, $CDCl_3$) δ 172.33, 171.35, 166.29, 160.95, 160.23, 156.99 (d, J = 245.7 Hz), 151.63, 142.76 (d, J = 9.9 Hz), 137.56, 134.58, 133.17, 132.33 (d, J = 9.8 Hz), 128.30, 127.85, 127.42 (q, J = 3.7 Hz), 126.88, 125.86, 125.22 (q, J = 32.8 Hz), 124.29, 124.28 (q, J = 271.4 Hz), 122.62, 121.95, 120.65 (d, J = 4.5 Hz), 119.98, 117.79, 116.84, 109.32 (d, J = 2.7 Hz), 102.49 (d, J = 24.6 Hz), 64.45, 55.10, 53.53, 51.38, 50.16, 31.23, 25.73, 23.23. LRMS (ESI) *m/z*: 755.4 $[M + H]^+$. HRMS (ESI): *m/z* calcd for $C_{41}H_{39}F_4N_6O_4^+$ $[M + H]^+$, 755.2969; found, 755.2957.

N-((1R)-1-(6-((4-(2-(2,6-dioxopiperidin-3-yl)-1-oxoisoindolin-5-yl)piperazin-1-yl)methyl)pyridin-2-yl)ethyl)-5-(4-(trifluoromethyl)phenoxy)-2-naphthamide (**HC278-Neg1**). Compound **HC278-Neg1** was synthesized from **35** and **50b** using a similar procedure for the preparation of compound **13**. It was obtained as a white solid (5.8 mg, 35 % yield). ^{1}H NMR (600 MHz, Chloroform-*d*) δ 8.51–8.44 (m, 1H), 8.27 (d, J = 8.5 Hz, 1H), 8.16–8.11 (m, 1H), 8.09 (d, J = 7.1 Hz, 1H), 7.93 (dd, J = 8.8, 1.7 Hz, 1H), 7.79 (dd, J = 8.3, 1.3 Hz, 1H), 7.73–7.67 (m, 2H), 7.57 (d, J = 8.6 Hz, 2H), 7.50–7.44 (m, 1H), 7.41–7.36 (m, 1H), 7.23 (d, J = 7.7 Hz, 1H), 7.15–7.10 (m, 1H), 7.05 (d, J = 8.5 Hz, 2H), 6.92 (dt, J = 8.7, 2.6 Hz, 1H), 6.82 (t, J = 2.4 Hz, 1H), 5.44–5.35 (m, 1H), 5.22–5.14 (m, 1H), 4.37 (d, J = 15.6 Hz, 1H), 4.22 (d, J = 15.6 Hz, 1H), 3.86–3.73 (m, 2H), 3.31 (t, J = 5.0 Hz, 4H), 2.92–2.65 (m, 6H), 2.34–2.24 (m, 1H), 2.20–2.16 (m, 1H), 1.62 (d, J = 6.8 Hz, 3H). ^{13}C NMR (150 MHz, $CDCl_3$) δ 171.39, 169.97, 169.96, 169.64, 166.28, 160.87, 160.40, 157.67, 154.50, 151.66, 143.76, 137.65, 134.55, 133.13, 128.28, 127.85, 127.44 (q, J = 3.7 Hz), 126.95, 126.93, 125.77, 125.29 (q, J = 32.8 Hz), 125.14, 124.26 (q, J = 271.4 Hz), 124.25, 122.62, 122.00, 121.84, 120.09, 117.81, 116.86, 116.84, 115.59, 108.43, 64.32, 53.06, 51.85, 50.20, 48.45, 47.02, 31.73, 23.59, 23.17. LRMS (ESI) *m/z*: 777.3 $[M + H]^+$. HRMS (ESI): *m/z* calcd for $C_{43}H_{40}F_3N_6O_5^+$ $[M + H]^+$, 777.3012; found, 777.3001.

Tert-butyl 4-(2-(1-methyl-2,6-dioxopiperidin-3-yl)-1-oxoisoindolin-5-yl)piperazine-1-carboxylate (**55**). To a solution of compound **34** (50 mg, 0.116 mmol) in DMSO (2 mL) was added MeI **54** (18.22 mg, 0.128 mmol), and K_2CO_3 (32.25 mg, 0.233 mmol). The resulting mixture was stirred at room temperature for 2 h. After completion of the reaction by checking the thin layer chromatography, the mixture was extracted with EtOAc. The combined organic layers were washed with brine and then concentrated. The residue was purified by flash column chromatography (0 %–90 % of EtOAc in hexanes) to afford compound **55** (44 mg, 86 % yield) as a white solid. ^{1}H NMR (600 MHz, Chloroform-*d*) δ 7.74 (d, J = 8.5 Hz, 1H), 6.98 (dd, J = 8.6, 2.2 Hz, 1H), 6.87 (d, J = 2.2 Hz, 1H), 5.15 (dd, J = 13.5, 5.0 Hz, 1H), 4.38 (d, J = 15.6 Hz, 1H), 4.25 (d, J = 15.6 Hz, 1H), 3.59 (t, J = 5.2 Hz, 4H), 3.31–3.23 (m, 4H), 3.17 (s, 3H), 3.00–2.94 (m, 1H), 2.88–2.80 (m, 1H), 2.33–2.24 (m, 1H), 2.18–2.13 (m, 1H), 1.48 (s, 9H). LRMS (ESI) *m/z*: 443.1 $[M + H]^+$.

N-((1S)-1-(6-((4-(2-(1-methyl-2,6-dioxopiperidin-3-yl)-1-oxoisoindolin-5-yl)piperazin-1-yl)methyl)pyridin-2-yl)ethyl)-5-(4-(trifluoromethyl)phenoxy)-2-naphthamide (**HC278-Neg2**). Compound **HC278-Neg2** was synthesized from **50a** and **55** using a similar procedure for the preparation of compound **11**. It was obtained as a white solid (13.7 mg, 80 % yield). ^{1}H NMR (600 MHz, Chloroform-*d*) δ 8.49 (d, J = 1.8 Hz, 1H), 8.16 (dd, J = 8.7, 1.1 Hz, 1H), 8.11 (d, J = 7.1 Hz, 1H), 7.95 (dd, J = 8.8, 1.7 Hz, 1H), 7.85–7.78 (m, 1H), 7.76–7.69 (m, 2H), 7.60 (d, J = 8.5 Hz, 2H), 7.49 (t, J = 7.9 Hz, 1H), 7.41 (dd, J = 7.7, 1.0 Hz, 1H), 7.25 (d, J = 7.7 Hz, 1H), 7.18–7.13 (m, 1H), 7.08 (d, J = 8.5 Hz, 2H), 6.95 (dt, J = 8.6, 2.8 Hz, 1H), 6.85 (t, J = 2.7 Hz, 1H), 5.48–5.37 (m, 1H), 5.17 (dd, J = 13.5, 5.0 Hz, 1H), 4.37 (dd, J = 15.7, 2.0 Hz, 1H), 4.24 (d, J = 15.6 Hz, 1H), 3.89–3.74 (m, 2H), 3.34 (t, J = 5.0 Hz, 4H), 3.19 (d, J = 2.2 Hz, 3H), 3.04–2.95 (m, 1H), 2.92–2.82 (m, 1H), 2.74 (t, J = 5.0 Hz, 4H), 2.34–2.23 (m, 1H), 2.21–2.13 (m, 1H), 1.65 (d, J = 6.8 Hz, 3H). ^{13}C NMR (150 MHz, $CDCl_3$) δ 171.52, 170.51, 169.72, 166.28, 160.88, 160.38, 157.71, 154.48, 151.68, 143.80, 137.67, 134.56, 133.15, 128.30, 127.85, 127.45 (q, J = 3.8 Hz), 126.96, 125.76, 125.31 (q, J = 32.6 Hz), 125.15, 124.27 (q, J = 271.6 Hz), 124.25, 122.64, 122.29, 121.84, 120.10, 116.86, 116.84, 115.63, 108.48, 64.37, 53.10, 52.53, 50.19, 48.53, 47.20, 32.25, 27.27, 23.22, 22.98. LRMS (ESI) *m/z*: 791.2 $[M + H]^+$. HRMS (ESI): *m/z* calcd for $C_{44}H_{42}F_3N_6O_5^+$ $[M + H]^+$, 791.3169; found, 791.3158.

N-(3-(2-(methylamino)-2-oxoethyl)benzyl)-5-(4-(trifluoromethyl)phenoxy)-2-naphthamide (**15**). Compound **15** was synthesized from **25** and Methylamine **56** using a similar procedure for the preparation of compound **1**. It was obtained as a white solid (19.0 mg, 93 % yield). ^{1}H NMR (600 MHz, Chloroform-*d*/CD_3OD 30/1) δ 8.40 (d, J = 1.8 Hz, 1H), 8.09 (d, J = 8.8 Hz, 1H), 7.86 (dd, J = 8.8, 1.8 Hz, 1H), 7.76 (d, J = 8.3 Hz, 1H), 7.56 (d, J = 8.6 Hz, 2H), 7.47 (t, J = 7.9 Hz, 1H), 7.36 (t, J = 5.7 Hz, 1H), 7.32–7.26 (m, 2H), 7.25–7.22 (m, 1H), 7.15 (dt, J = 7.1, 1.9 Hz, 1H), 7.12 (d, J = 7.5 Hz, 1H), 7.04 (d, J = 8.5 Hz, 2H), 5.92 (s, 1H), 4.65 (d, J = 5.5 Hz, 2H), 3.50 (s, 2H), 2.72 (d, J = 4.9 Hz, 3H). ^{13}C NMR (150 MHz, Chloroform-*d*/CD_3OD 30/1) δ 172.10, 167.65, 160.81, 151.63, 139.01, 135.46, 134.46, 132.48, 129.41, 129.02, 128.64, 128.33, 127.88, 127.40 (q, J = 3.8 Hz), 126.96, 126.93, 125.72, 125.29 (q, J = 32.7

Hz), 124.22 (q, $J = 271.5$ Hz), 124.20, 122.66, 117.80, 116.89, 44.17, 43.45, 26.62. LRMS (ESI) *m/z*: 493.2 $[M + H]^+$. HRMS (ESI): *m/z* calcd for $C_{28}H_{24}F_3N_2O_3^+$ $[M + H]^+$, 493.1739; found, 493.1732.

(S)-N-(1-(pyridin-2-yl)ethyl)-5-(4-(trifluoromethyl)phenoxy)-2-naphthamide (**Ex. 29**). Compound **Ex. 29** was synthesized from **23** and (S)-1-(pyridin-2-yl)ethan-1-amine **57** using a similar procedure for the preparation of compound **1**. It was obtained as a white solid (64.0 mg, 97 % yield). ^{1}H NMR (600 MHz, Chloroform-*d*) δ 8.63–8.57 (m, 1H), 8.45 (d, $J = 1.7$ Hz, 1H), 8.12 (d, $J = 8.7$ Hz, 1H), 8.00–7.89 (m, 2H), 7.82 (d, $J = 8.3$ Hz, 1H), 7.71 (td, $J = 7.6$, 1.8 Hz, 1H), 7.62–7.55 (m, 2H), 7.51 (t, $J = 7.9$ Hz, 1H), 7.33 (dt, $J = 7.8$, 1.2 Hz, 1H), 7.26–7.21 (m, 1H), 7.14 (dd, $J = 7.5$, 1.0 Hz, 1H), 7.10–7.03 (m, 2H), 5.45–5.36 (m, 1H), 2.80 (s, 1H), 1.63 (d, $J = 6.8$ Hz, 3H). ^{13}C NMR (150 MHz, $CDCl_3$) δ 166.34, 160.96, 151.61, 149.20, 137.13, 134.57, 133.09, 128.31, 127.77, 127.42 (q, $J = 3.8$ Hz), 126.85, 125.85, 125.24 (q, $J = 32.7$ Hz), 124.35, 124.28 (q, $J = 271.4$ Hz), 122.62, 121.77, 117.75, 116.89, 50.32, 23.15. LRMS (ESI) *m/z*: 437.2 $[M + H]^+$. HRMS (ESI): *m/z* calcd for $C_{25}H_{20}F_3N_2O_2^+$ $[M + H]^+$, 437.1477; found, 437.1470.

3. Results

3.1. Design and evaluation of novel TEAD-degrading PROTACs

Several TEAD palmitoylation inhibitors with diverse molecular structures have been discovered, but most of them exhibit non-significant selectivity among TEAD1-4 [21,22]. Given the differing mechanisms of action between inhibitors and degraders, our focus was on developing TEAD degraders with the capability to achieve isoform-selective degradation. The TEAD palmitoylation inhibitor VT3989 from Vivace Therapeutics is currently in Phase I clinical trials; however, its structure has not yet been disclosed [29]. We selected a highly potent and potentially drug-like TEAD inhibitor **Ex. 29** disclosed in a published patent by Vivace Therapeutics (Fig. S1A) [61]. This compound inhibits a YAP transcriptional reporter with an IC_{50} of less than 100 nM. Related analogs of **Ex. 29** are known to bind to all four TEAD paralogs with nanomolar affinity. Therefore, **EX. 29** is expected to bind the different TEAD paralogs

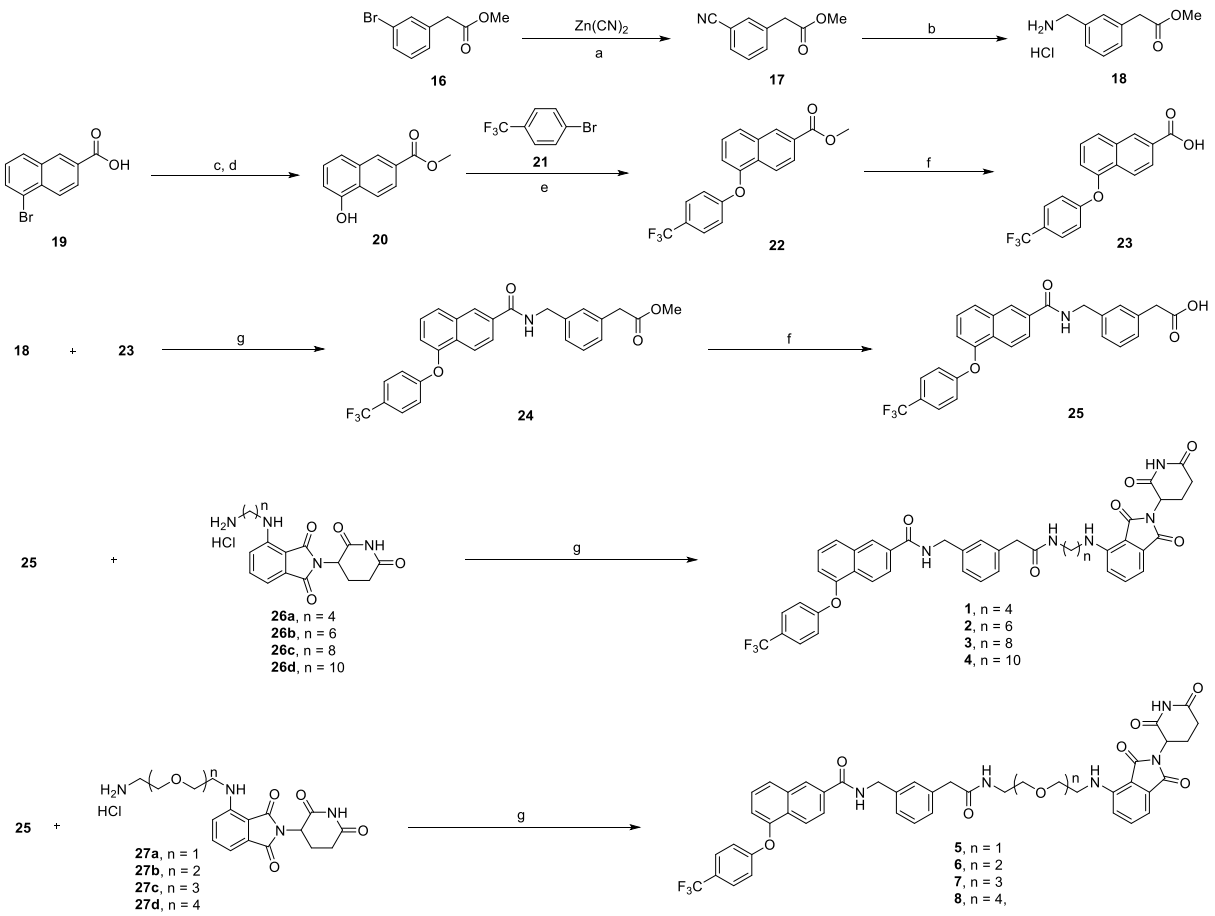

Scheme 1. Synthesis of compounds **1-8**[a].

[a] Reagents and conditions: (a) $Zn(CN)_2$, $Pd(PPh_3)_4$, DMF, 90 °C, 4 h; (b) H_2, 10 % Pd/C, 4 M HCl 1,4-dioxane, MeOH, rt, overnight; (c) Cu_2O, 4,7-dihydroxy-1,1′-phenanthroline, TBAOH (40 % in H_2O), H_2O, 100 °C, overnight; (d) $SOCl_2$, MeOH, 70 °C, 2 h; (e) $Pd(OAc)_2$, tBu-XPhos, K_3PO_4, toluene, 110 °C, overnight; (f) NaOH, MeOH/THF/H_2O, rt, 3 h; (g) HATU, DIEA, DMF, rt overnight.

with very high affinity. *In silico* docking studies indicated that the pyridine moiety of **Ex. 29** extends to the solvent-exposed area (Fig. S1B), highlighting the suitability of this pyridine site for attaching a linker to connect with an E3 ligase ligand, facilitating the development of PROTAC degraders. Due to the CRBN E3 ligase binders' low molecular weight and favorable drug-like properties, the design of the novel TEAD degraders involved linking compound **Ex. 29** with pomalidomide/lenalidomide through different linkers (Fig. S1C). These novel TEAD degraders were subsequently synthesized using different synthetic routes, which are outlined in Schemes 1–4.

In parallel, we developed a platform for screening the TEAD degrading activities of the PROTACs (Fig. 1A). The TEAD transcription factors exist in four different paralogs, making it important to determine whether a PROTAC can degrade all four of them or only specific paralogs. However, a major obstacle is that no single cell line naturally expresses all four TEAD paralogs in detectable amounts, which creates a challenge to assess PROTACs' ability to selectively degrade specific paralogs using available pan-TEAD antibodies. Further, the commercially available antibodies against different TEAD paralogs are not equally specific. To address this challenge, we engineered a construct encoding FLAG-tagged TEAD1, Myc-tagged TEAD2, V5-tagged TEAD3, and HA-tagged TEAD4, interspersed with viral 2A-like peptides in between (Fig. 1A). This allows translation of the four different proteins from a single transcript produced under the control of a single promoter, thus eliminating variability due to differing strengths of promoters. This construct successfully produces individually tagged TEAD1-4. Subsequently, we established a stable cell line harboring this construct, with one of the stable cell clones expressing all four TEAD paralogs, that can be readily detected by commercially available antibodies against the different epitope tags (Fig. 1B). Using this cell line, we screened the designed PROTACs at concentrations of 0.1 μM (Fig. S2).

3.2. The TEAD-degrading PROTACs potently degrade TEAD1 and TEAD3

Based on the screening results of all these fourteen compounds, we selected three PROTACs, **HC242**, **HC278**, and **HC286** for further characterization (Fig. 1C). To evaluate the potency of these PROTACs, we performed a dose-response analysis. The cells were treated with varying concentrations of the PROTACs, and the effect on all four TEAD paralogs was assessed by Western blotting, using antibodies against the respective epitope tags. These experiments revealed that while all three PROTACs **HC242**, **HC278**, and **HC286** can

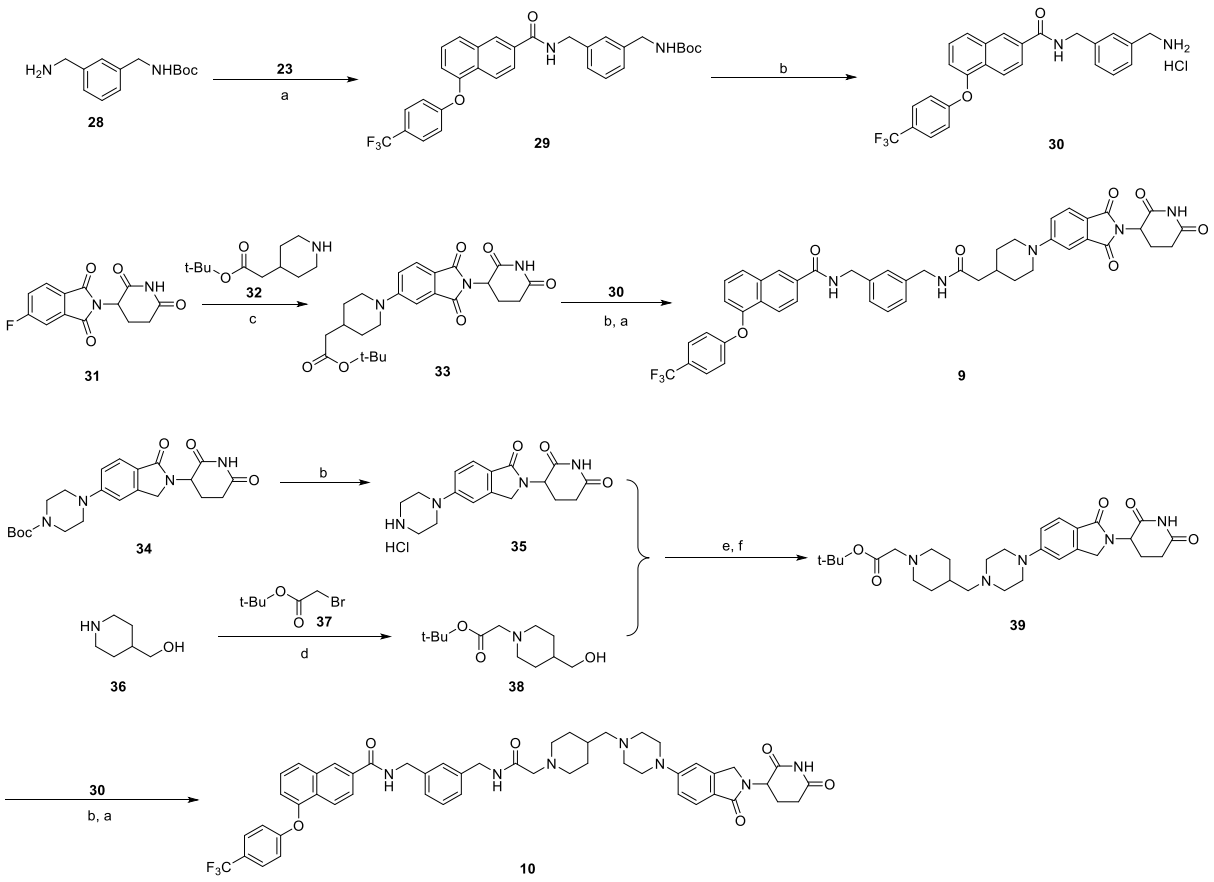

Scheme 2. Synthesis of compounds **9**–**10**[a]:
[a] Reagents and conditions: (a) HATU, DIEA, DMF, rt overnight; (b) 4 M HCl 1,4-dioxane, rt, 4 h; (c) DIEA, DMSO, 90 °C, overnight; (d) THF, rt, overnight; (e) Oxalyl chloride, DMSO, TEA, DCM, −78-rt, 3 h; (f) $NaBH_3CN$, KOAc, DCM/MeOH, rt, overnight.

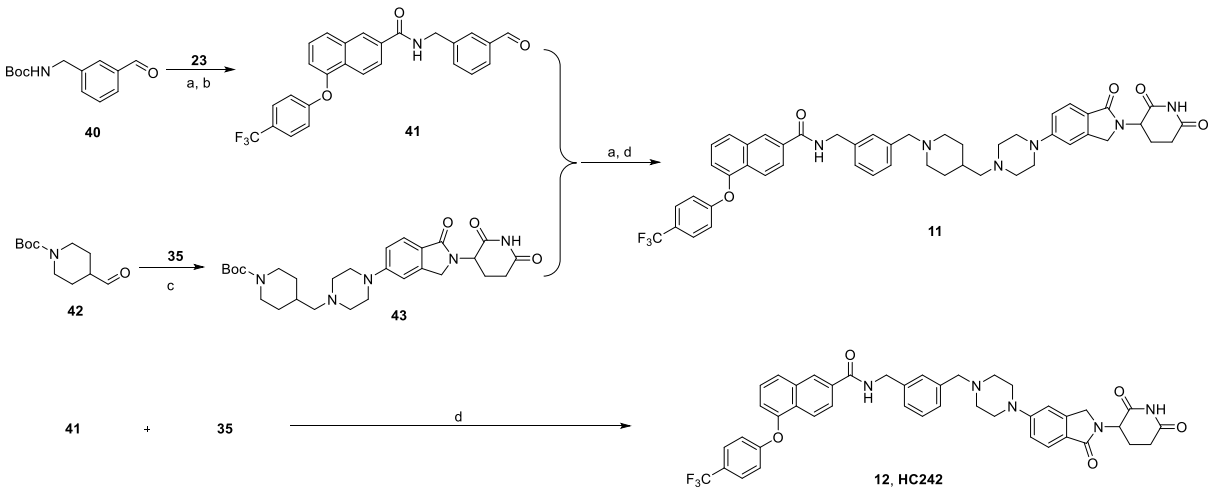

Scheme 3. Synthesis of compounds **11**–**12**[a]:
[a] Reagents and conditions: (a) 4 M HCl 1,4-dioxane, DCM, rt, 1 h; (b) HATU, DIEA, DMF, rt, 2 h; (c) $NaBH(OAc)_3$, DIEA, DMSO/DCM, rt, overnight; (d) $NaBH_3CN$, KOAc, MeOH/AcOH, rt, overnight.

degrade TEAD1 and TEAD3 even at 50 nM, they have little effect on TEAD2 and had only a weak degrading effect on TEAD4 at 500 nM, indicating that these PROTACs are more specific for TEAD1 and TEAD3 (Fig. 1D–F') at low doses. Since these PROTACs can cause more than 50 % degradation at 50 nM, we decided to determine their degradative effect on TEAD1 and TEAD3 at lower concentrations (Fig. S3). These experiments revealed that **HC242**, **HC278**, and **HC286** can degrade TEAD1 and TEAD3 at low nanomolar concentrations.

3.3. TEAD degrading PROTACs function in a proteasome and CRBN-dependent manner

To determine the kinetics of degradation by the PROTACs, we treated the HEK293-pan-TEAD cells with 500 nM **HC242**, **HC278,** and **HC286** for different time periods and assessed TEAD degradation by Western blotting (Fig. S4). TEAD1/3 degradation could be detected as early as 2 h after PROTAC treatment and continued to increase over time. We further performed rescue experiments to investigate whether **HC242**, **HC278,** and **HC286** are bona fide PROTAC degraders. When cells co-treated with these PROTACs and the proteasomal inhibitor MG132, the degradation of TEAD proteins was completely blocked, suggesting that these compounds degrade TEAD proteins in a proteasomal-dependent manner (Fig. 2A–C'). Similarly, co-treatment of the cells with the warheads, **15** and **Ex. 29** also inhibited the degradation activity of the PROTACs on TEAD proteins, suggesting that the warhead of the PROTACs engaged with the TEAD proteins (Fig. 2A–C'). Furthermore, the negative control **HC278-Neg1**, in which the TEAD binding warhead is the enantiomer of the one in **HC278**, exhibited a much weaker degradative effect (Fig. 2D and E). Another negative control, **HC278-Neg2**, uses the same warhead as in **HC278** but contains an altered CRBN ligand that cannot engage with CRBN, failed to induce degradation of the TEAD proteins (Fig. 2D–F). This confirms that the activity of these PROTACs is CRBN-dependent. Taken together, these experiments revealed that **HC242**, **HC278**, and **HC286** are bona fide PROTAC degraders of TEAD1 and TEAD3.

3.4. HC278 can form ternary complex with TEAD1/3 and CRBN/DDB1

To gain more understanding of **HC278**-induced isoform selective degradation of TEAD proteins, we measured the in vitro formation of ternary complexes between CRBN/DDB1, **HC278,** and TEAD1-4, using the cell-free AlphaLISA assay [62]. For this, we used GST-tagged TEAD proteins and His-tagged CRBN/DDB1 (Fig. 3A). Since recombinant TEAD purified from *E. coli* is normally bound to palmitic acid, which would prevent binding of the PROTAC to TEAD, we purified the TEAD proteins with the conserved cysteine mutated to alanine. As expected, **HC278** can form stable ternary complexes with TEAD1 and CRBN/DDB1 complex, which is consistent with the Western blotting data (Fig. 3B). In contrast, **HC278-Neg1** generated a weak Alpha signal due to its reduced binding affinity to TEAD. Similarly, **HC278-Neg2,** which cannot bind to CRBN, also failed to form a stable ternary complex (Fig. 3B). Consistent with the isoform selectivity observed in the Western blotting assay, we found that TEAD1 and TEAD3 could form stable ternary complexes with **HC278** and CRBN/DDB1, whereas TEAD2 and TEAD4 weakly formed ternary complex (Fig. 3C). Taken together, these results suggest that **HC278**-induced paralog-selective TEAD degradation is derived from its ability to differentially promote ternary complex formation among the TEAD proteins.

3.5. HC278 selectively depletes TEAD1/3 in the whole proteome

To further investigate the degradation selectivity of **HC278** beyond the TEAD family of proteins, we performed an unbiased global

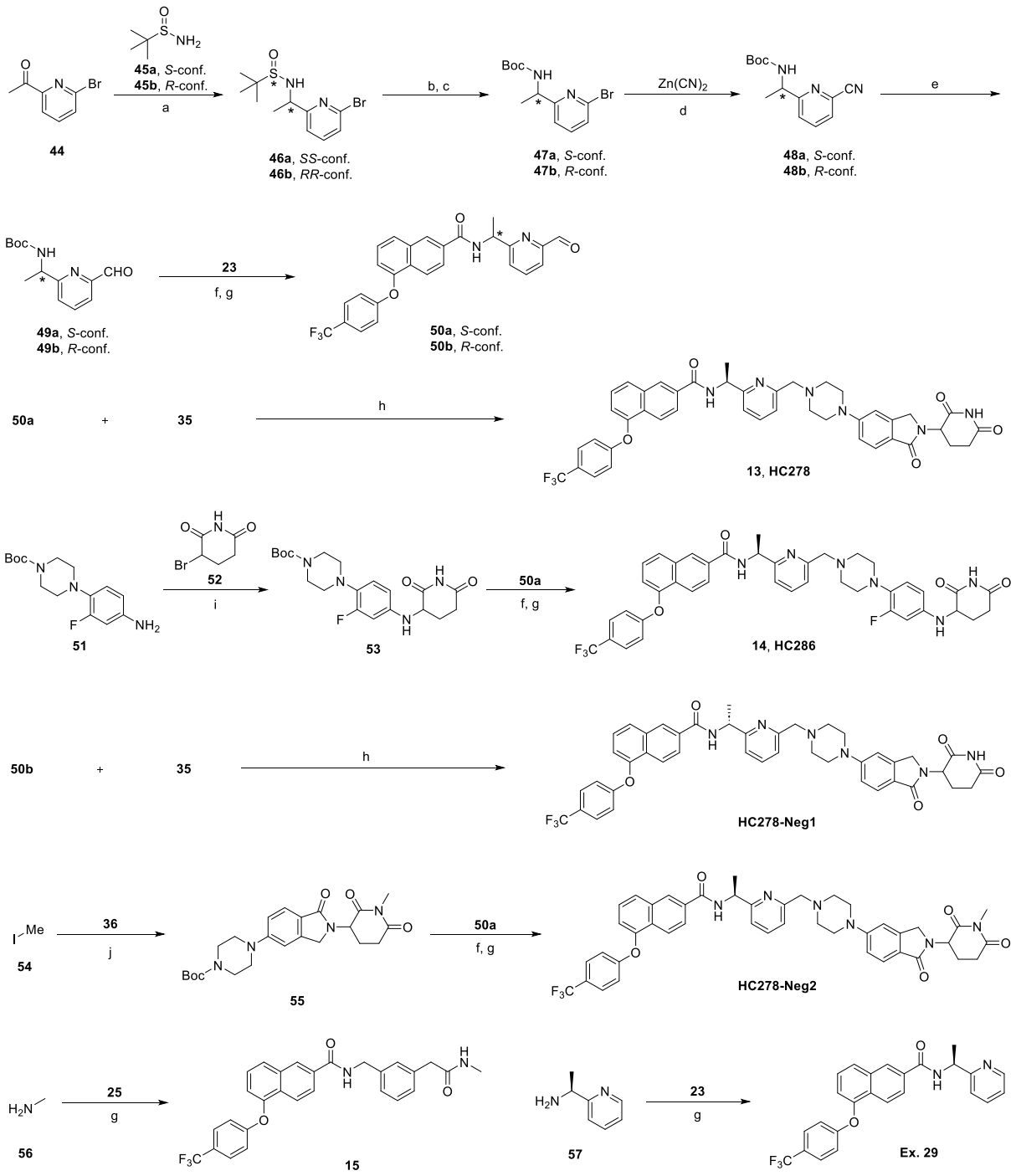

Scheme 4. Synthesis of compounds **13-Ex. 29**[a]:
[a] Reagents and conditions: (a) $Ti(OEt)_4$, $NaBH_4$, THF, 70 °C-rt, overnight; (b) 4 M HCl 1,4-dioxane, MeOH, rt, 1 h; (c) Boc_2O, DIEA, DCM, rt, 1 h; (d) $Zn(CN)_2$, $Pd(PPh_3)_4$, DMF, 100 °C, 8 h; (e) DIBAL-H, DCM. −78 °C, 4 h; (f) 4 M HCl 1,4-dioxane, DCM, rt, 1 h; (g) HATU, DIEA, DMF, rt, 2 h; (h) $NaBH_3CN$, KOAc, MeOH/AcOH, rt, overnight; (i) DIEA, DMSO, 70 °C, overnight; (j) K_2CO_3, DMSO, rt, 2 h.

proteomic analysis. We treated NCI-H226 cells with either DMSO or 500 nM of **HC278** for 24 h, extracted total protein and identified the proteins up or downregulated by **HC278** treatment. We observed significant downregulation of TEAD1 and TEAD3 (Fig. 4A and B and Fig. S5), while TEAD2 was not detectable, presumably because it is not expressed in these cells. Consistent with these findings, Western blotting analysis of the cell lysates from NCI-H226 cells treated with either DMSO or 100 and 500 nM of **HC278** for 24 h

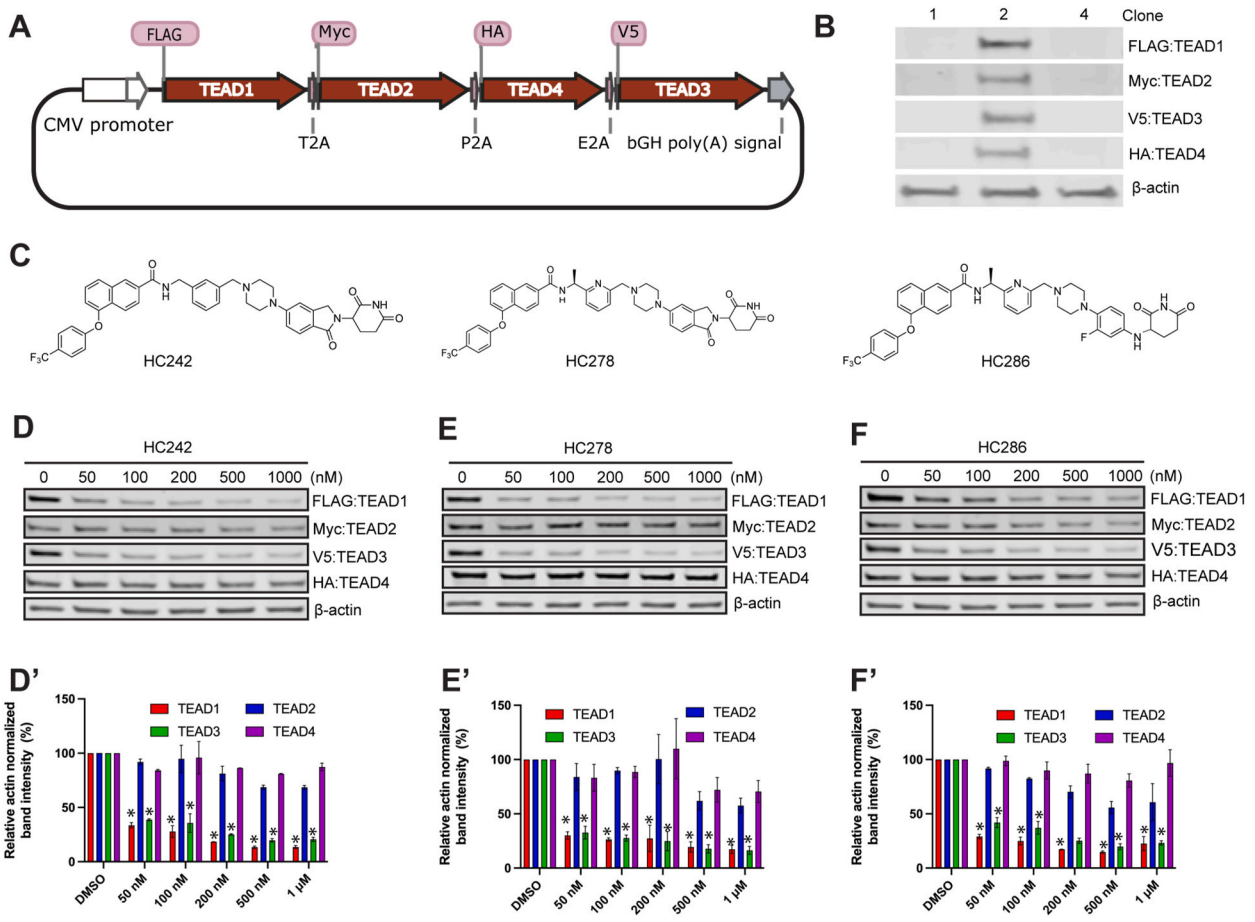

Fig. 1. HC242, HC278, and HC286 selectively degrades TEAD1 and TEAD3
(A) A schematic of the pTRE-panTEAD plasmid showing TEAD1-4 with FLAG, MYC, HA, and V5 tags interspersed with T2A, P2A, and E2A coding sequences to produce epitope-tagged TEAD paralogs from a single transcript produced from the CMV promoter.
(B) Western blotting showing isolation of a stable cell clone that expresses FLAG-TEAD1, MYC-TEAD2, V5-TEAD3, and HA-TEAD4.
(C) Chemical structure of **HC242**, **HC278**, and **HC286**.
(D-F′) Representative Western blots (D–F) and histograms (D′-F′) showing dose-dependent degradation of TEAD by **HC242**, **HC278,** and **HC286**. HEK293 stable cells expressing epitope-tagged TEAD1-4, were treated with indicated doses of **HC242**, **HC278,** and **HC286** for 18 h, and the level of TEAD1-4 was detected by Western blotting using antibodies against the corresponding epitope tags. Actin was used as a control for loading, transfer, and normalization. Histograms show mean ± SEM (n = 3). *: $p < 0.05$.

revealed that TEAD1 and TEAD3 are significantly degraded by 100 nM of **HC278** (Fig. 4E and F)**.** In contrast, TEAD4 was only mildly degraded even at 500 nM dose of **HC278.** Consistent with the proteomics result, we could not detect TEAD2 in these cells. **HC242** and **HC286** also exhibited a similar degradative effect on different TEAD isoforms (Figs. S5A–D) In addition, we observed that several other proteins including INHBA, ADAMTS1, F3, and ZNF367 were downregulated. This could be due to the fact that they are transcriptional targets of TEAD/YAP. To address this possibility, we treated the NCI-H226 cells with either DMSO or 500 nM **HC278** for 24 h, following which we isolated the RNA and performed RNA Sequencing (RNA-Seq) analysis to examine the effect of this PROTAC on the global transcriptome. Consistent with our predictions, proteins such as INHBA, ADAMTS1, F3, and ZNF367 that were downregulated in the proteomics experiment were also downregulated in the RNA-seq experiment, indicating that the downregulation of these proteins in response to **HC278** treatment is due to inhibition of TEAD transcriptional effect (Fig. 4C and D). Recently, a PROTAC developed from a TEAD palmitoylation inhibitor was reported to induce the degradation of PDCD2 [63]. However, our proteomics data showed that **HC278** does not cause PDCD2 degradation. This was further confirmed by Western blotting (Fig. S6). These results also indicate that **HC278** specifically depletes TEAD1/3 and to a lesser extent TEAD4 and downregulates their transcriptional targets.

3.6. HC278 downregulates TEAD/YAP-regulated transcriptome

Given that **HC278** depletes TEAD1 and TEAD3 and degrades TEAD4 to some extent, we predicted that it would inhibit TEAD/YAP transcriptional activity. To address this possibility, we further analyzed our RNA-Seq data by comparing it with published YAP signature data sets. Overall, a small set of genes was found to be downregulated or upregulated by > 2 fold ($p < 0.05$) in cells treated

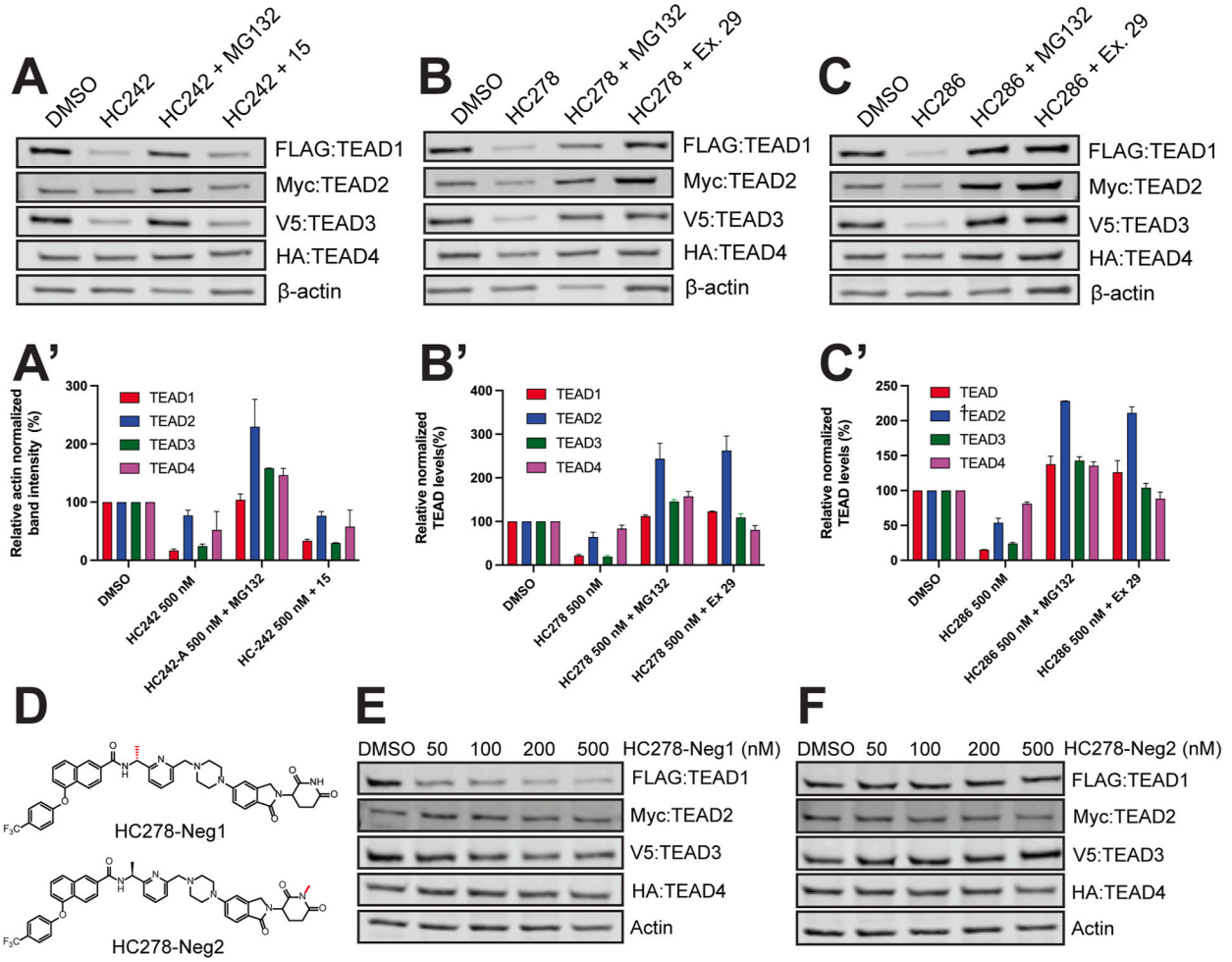

Fig. 2. TEAD degrading PROTACs function in proteasome and CRBN-dependent manner
(A-C′) Representative Western Blots (A–C) and histograms (A′-C′) showing inhibition of **HC242**-induced TEAD degradation by MG132 and the warhead **15** (A, A′) or **Ex. 29** (B-C′). HEK293 stable cells expressing epitope-tagged TEAD1-4, treated with DMSO, or 500 nM **HC242** (A, A′), **HC278** (B, B′) or **HC286** (C, C′) without or with 1 μM MG132 or 500 nM **15** or **Ex. 29** for 18 h, and the level of TEAD1-4 was detected by Western blotting using antibodies against the corresponding epitope tags. Actin was used as a control for loading and transfer. Histograms show mean ± SEM (n = 3).
(D) Chemical structures of the negative controls **HC278-Neg1** and **HC278-Neg2**.
(E, F) HEK293 stable cells expressing epitope-tagged TEAD1-4 were treated with indicated doses of **HC278-Neg1** (E) or **HC278-Neg2** (F) for 18 h and the level of TEAD1-4 was detected by Western blotting using antibodies against the corresponding epitope-tags. Actin was used as a control for loading and transfer.

with **HC278** compared to those treated with DMSO (Fig. 5A). Gene Set Enrichment Analysis (GSEA) of the differentially expressed genes revealed that several gene sets in the MSigDB oncogene dataset were highly enriched (Fig. 5B). Specifically, the Cordonensi YAP signature gene set is highly downregulated in the differentially expressed genes in cells treated with **HC278** (Fig. 5B and C). Consistently, a significant number of YAP-target genes such as CTGF, CYR61, and ANKRD1 were significantly downregulated (Fig. 5A). To further verify the RNA-Seq results, we examined the transcript levels for well-known YAP target genes such as CTGF, CYR61, and ANKRD1 by quantitative RT-PCR. Consistent with our RNA-seq analysis, the mRNA levels of CTGF, CYR61, and ANKRD1 were significantly downregulated in NCI-H226 cells treated with **HC278** compared to cells treated with DMSO (Fig. 5D). Taken together, these results demonstrate that **HC278** inhibits TEAD/YAP transcriptional activity.

3.7. The TEAD-degrading PROTACs inhibit growth of NCI-H226 cells

Inhibition of YAP transcriptional activity by **HC278** suggested that it can potentially inhibit the proliferation of YAP-driven cancer cells. HCNCI-HC226 mesothelioma cells harbor deletions in NF2, causing activation of YAP. Genetic studies have established that they exhibit vulnerability to loss of YAP/TEAD activity. Furthermore, several TEAD palmitoylation inhibitors are known to inhibit the proliferation of these cells. To determine how **HC278** affects growth of NCI-HC226 cells, a small number of cells were plated and

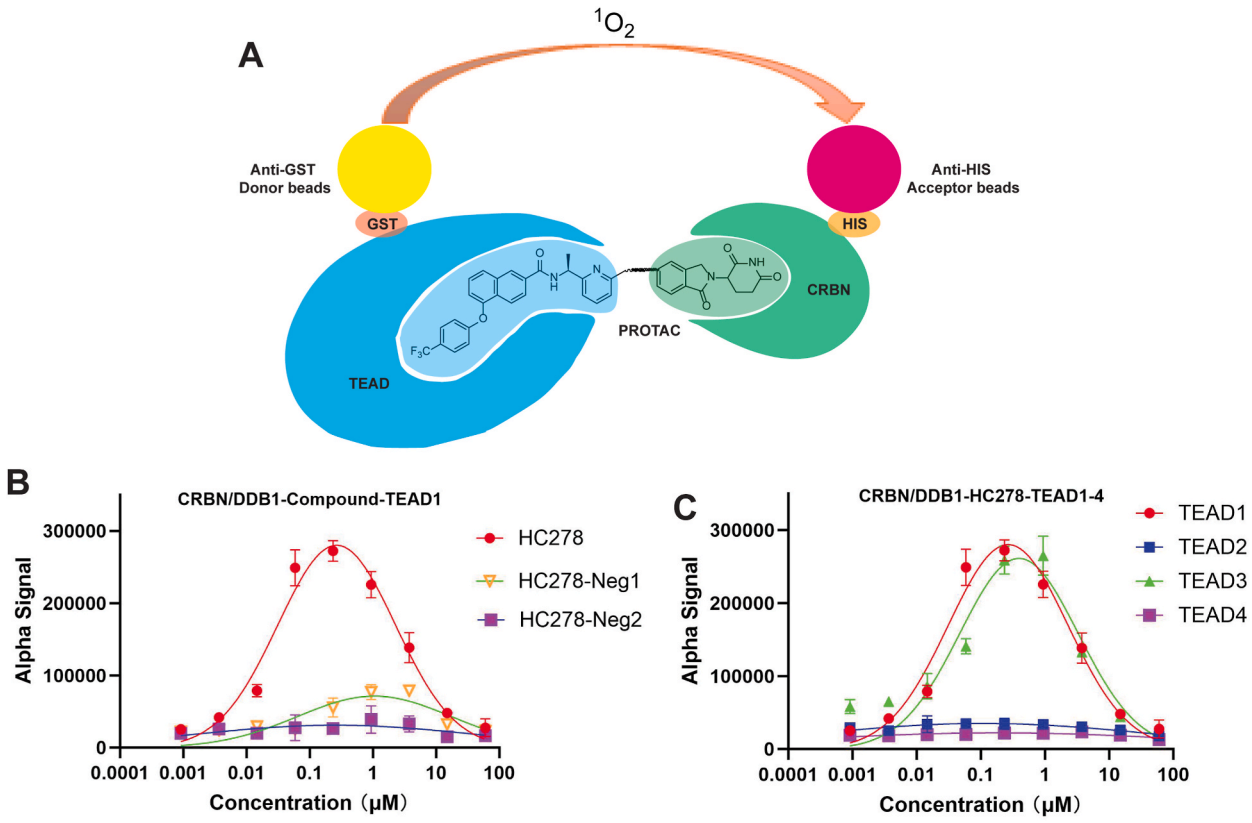

Fig. 3. HC278 induces ternary complex formation between TEAD1/3 and CRBN/DDB1
(A) Schematic illustration of the ternary complex formation assay using AlphaLISA assay.
(B, C) Ternary complex formation between the CRBN/DDB1, compounds, and TEAD1 (B) or TEAD1-4 based on in vitro AlphaLISA assay. Data are shown as mean ± SEM (n = 3).

treated with DMSO or 100 and 200 nM of **HC242**, **HC278**, and **HC286** for a week, and the colony size was quantified. These experiments revealed that **HC278** and **HC286** significantly inhibited colony forming ability of NCI-H226 cells at 200 nM (Fig. 6A–C) while had little effect at 100 nM dose. In contrast, the PROTACs had no apparent effect on the colony-forming ability of the NCI-H28 control mesothelioma cells that do not have mutations in Hippo pathway components (Fig. 6D–F), even at 200 nM dose. Together, these results indicate that these PROTACs specifically inhibit colony forming ability of YAP-dependent mesothelioma cells.

4. Discussion

The oncogenic transcriptional activators YAP/TAZ function as the terminal effectors of the Hippo signaling pathway and are frequently hyperactivated in many human cancers. Thus, they provide a critical point for therapeutic intervention in cancers. YAP/TAZ exert their oncogenic activity by regulating gene expression by associating primarily with the TEAD transcription factors. Thus, YAP activity can be impaired by inhibiting TEAD. The TEAD transcription factors exist as four different paralogs TEAD1-4, which are highly similar in sequence and structure. A unique feature of TEAD proteins is that they get autopalmitoylated, and inhibiting this posttranslational modification interferes with their function. Therefore, several TEAD palmitoylation inhibitors have been developed over the last few years. A few of these have even entered clinical trials. However, it has been reported that cancer cells can rapidly develop resistance, which could limit their effectiveness. In some cases, the resistance is mediated by TEAD binding partner and transcriptional corepressors VGLL3. Consequently, degrading TEAD through proximity induced ubiquitination would be an attractive alternative approach. In this study, we developed and characterized PROTACs that can potently degrade TEAD1 and TEAD3 at low nanomolar concentrations while degrading TEAD2 and 4 only at higher doses. These molecules degrade TEAD in a proteasome and CRBN-dependent manner and inhibit YAP transcriptional response. Consistently they exhibit antiproliferative effects on the YAP-dependent mesothelioma cells. This has important biological and clinical implications for treatment of disease conditions that are primarily dependent on TEAD1 and TEAD3. Moreover, it is conceivable to develop PROTACs that specifically degrade TEAD2 and TEAD4 and use them in combination with **HC278** to deplete all four TEADs. Interestingly, a TEAD2 specific degrader was recently published [64]. Further investigations will be required to determine if the TEAD degraders have an advantage over the autopalmitoylation inhibitors with respect to the development of resistance.

To study the paralog-specific effect of PROTACs we created a stable cell line that expresses the different TEAD paralogs with unique

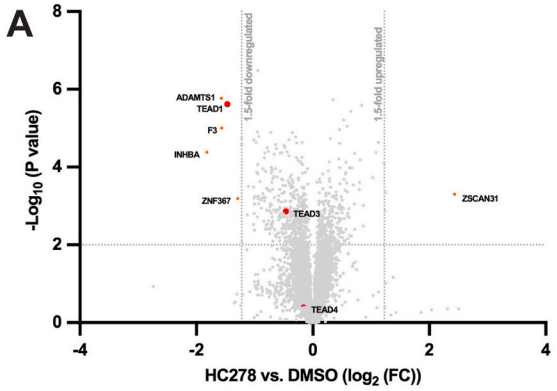

B

NCI-H226			
Gene	Log_2 (FC)	P-value	$-Log_{10}$ P-value
TEAD1	-1.47	2.41E-06	5.62
TEAD3	-0.46	1.40E-03	2.86
TEAD4	-0.16	4.04E-01	0.39
ADAMTS1	-1.57	1.69E-06	5.77
F3	-1.57	9.88E-06	5.01
INHBA	-1.82	4.16E-05	4.38
ZNF367	-1.29	6.48E-04	3.19
ZSCAN31	2.43	4.99E-04	3.30

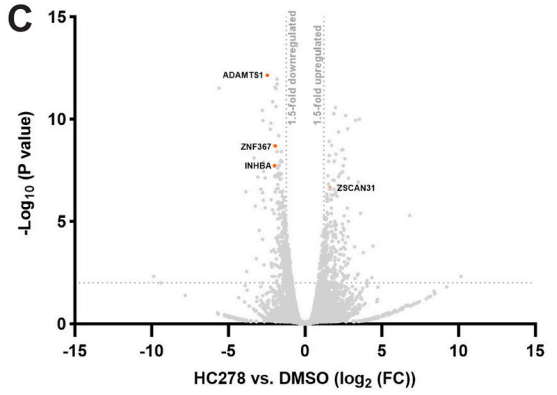

D

NCI-H226			
Gene	Log_2 (FC)	P-value	$-Log_{10}$ P-value
ADAMTS1	-2.46	7.13E-13	12.15
INHBA	-2.00	1.85E-08	7.73
ZNF367	-1.94	2.00E-09	8.70
ZSCAN31	1.61	2.28E-07	6.64

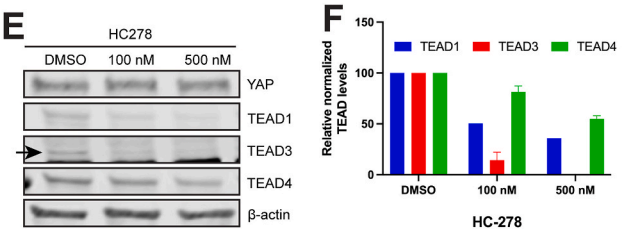

Fig. 4. Proteomic and RNA-seq profiling of HC278-mediated degradation
(A) A scatterplot depicting the log2 (Fold Change) of relative protein abundance in NCI-H226 cells treated with **HC278** (500 nM, 24 h) compared to those treated with DMSO in TMT proteomic profiling.
(B) Top hits identified by TMT (A) proteomic profiling.
(C) A scatterplot depicting the log2 (Fold Change) of relative protein abundance in NCI-H226 cells treated with **HC278** (500 nM, 24 h) compared to those treated with DMSO in RNA-seq profiling.
(D) Top hits identified by RNA-seq profiling (C).
(E–F) Representative Western Blot and Histograms showing the effect of 100 nM and 500 nM **HC278** on different TEAD paralogs and YAP in NCI-H226 cells treated for 18 h. Actin was used as the control for loading, transfer, and normalization. Histograms depict mean ± SEM (n = 3).

epitope tags. Currently, most studies on TEAD use the commercially available pan-TEAD antibody, which does not provide any information about specific effects on any TEAD paralogs. Similarly, the commercially available antibodies against the different paralogs are not very specific. Transient transfection with individual epitope-tagged TEAD paralog also introduces error due to variable transfection efficiency. Thus, our stable cell line will be an extremely valuable tool for high throughput screening to detect the paralog-specific degrading activity of small molecule degraders.

Our mechanistic studies revealed that our lead PROTAC, **HC278**, is capable of forming a stable ternary complex with CRBN/DDB1 and either TEAD1 or TEAD3 but not with TEAD2 or TEAD4. Forming a stable ternary complex is essential for PROTACs to trigger ubiquitination of their targets, though may not be the only requirement [65,66]. Thus, the isoform-selective degradation observed with our PROTACs towards TEAD1/3 could be attributed to their differential efficiency in inducing the formation of TEAD:PROTAC:CRBN/DDB1 ternary complex across the TEAD paralogs. It should be noted that PROTACs developed from non-selective ligands can degrade specific paralogs depending on the linker length, type, and geometry of orientation, which together can affect stable ternary complex formation. The TEAD2-specific degrader that was published recently uses a ligand known to bind to all four TEAD paralogs [64]. However, the PROTAC can specifically degrade TEAD2. Further studies are needed to elucidate the structural basis that governs the ternary complex formation.

Proteome-wide analysis revealed that **HC278** specifically degrades TEAD1 and TEAD3. We also observed several other proteins were downregulated with **HC278** treatment. However, transcriptome analysis revealed that these proteins were transcriptionally regulated by TEAD. Further, GSEA revealed that the YAP signature gene set was specifically downregulated upon **HC278** treatment, indicating that **HC278** specifically inhibits YAP transcriptional activities. Collectively our study identified potent and specific PROTAC degraders for TEAD1 and TEAD3, which will be valuable tools to study the biological functions of these TEAD paralogs and their

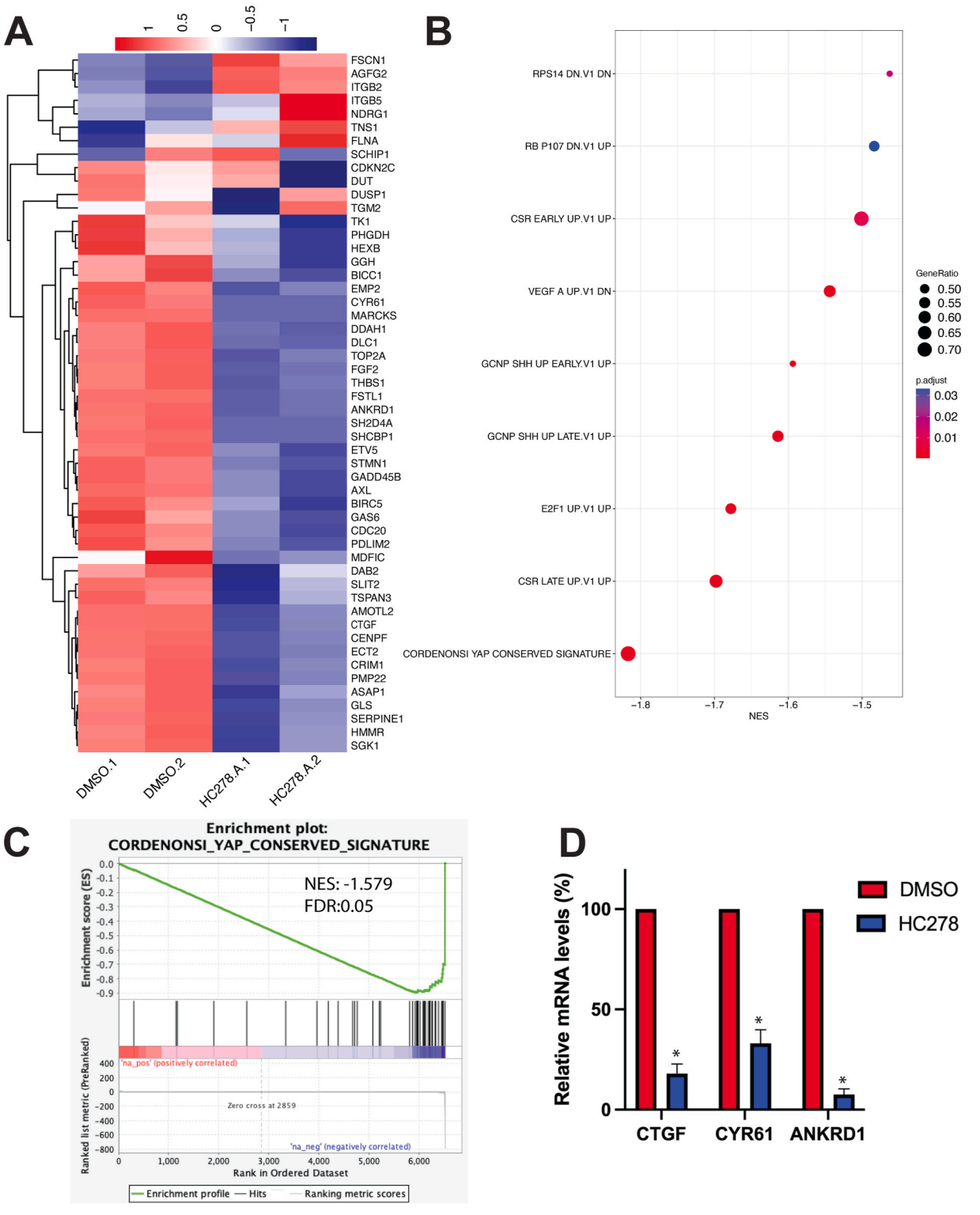

(caption on next page)

Fig. 5. TEAD-degrading PROTACs inhibit YAP transcriptional activity
(A) Heatmap showing transcripts upregulated (red) and downregulated (blue) in NCI-H226 cells treated with 500 nM of **HC278** for 24 h
(B) GSEA Enrichment plot of Differentially expressed genes in the MSigDB oncogenes
data set.
(C) Enrichment plot for Gene Set Enrichment Analysis for YAP signature gene set.
(D) Histograms showing relative expression of CTGF, CYR61, and ANKRD1 mRNA levels in NCI-H226 cells treated with DMSO or indicated doses of **HC278**. Data are shown as mean ± SEM (n = 3). * = $p < 0.05$. (For interpretation of the references to color in this figure legend, the reader is referred to the Web version of this article.)

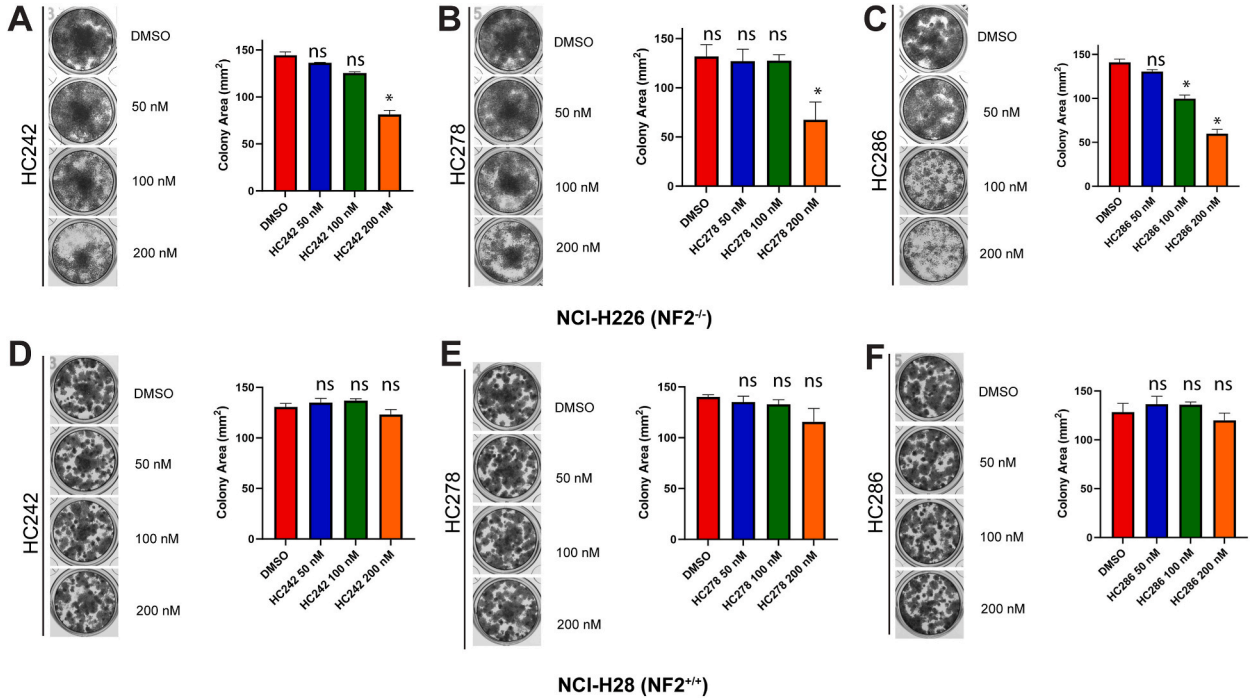

Fig. 6. TEAD-degrading PROTACs inhibit the colony forming ability of NCI-H226 cells
(A, F) Representative images and histograms showing colony formation assay for NCIH226 (A–C) or NCI-H28 (D–F) control cells, treated with DMSO or indicated doses of **HC242** (A, D), **HC278** (B, E) or **HC286** (C, F). Histograms show normalized colony area for DMSO and **HC242** treated NCI-H226 and NCI-H28 cells. (n = 3). *: $p < 0.05$, ns: Not significant.

potential in treating disease conditions specifically driven by them.

Funding sources

This research was supported in part by US National Institute of Health (NIH) grants R01 CA242003 (to GZ), R01241191 (to GZ), and Start-up funds from University of Texas at Dallas and Stony Brook University (to JRM).

Materials availability

Requests for resources and reagents should be directed to the Lead Contact: Jyoti R. Misra (jyoti.misra@stonybrook.edu). The reagents generated in this study will be made available subject to a completed Materials Transfer Agreement.

Data and code availability

(1) The transcriptomic profiling datasets data have been deposited at the Gene Expression Omnibus (GEO) (accession number: GSE255974). The mass spectrometry proteomics have been deposited at the Mass Spectrometry Interactive Environment (massive) (accession number: MSV000094099)
(2) This paper does not report original code.
(3) Any additional information required to reanalyze the data reported in this paper is available from the lead contact upon request.

CRediT authorship contribution statement

Hui Chen: Writing – original draft, Visualization, Validation, Methodology, Investigation, Conceptualization. **Artem Gridnev:** Writing – original draft, Visualization, Validation, Methodology, Investigation. **Netanya Schlamowitz:** Methodology, Investigation. **Wanyi Hu:** Methodology, Investigation. **Kuntala Dey:** Methodology, Investigation. **Guangrong Zheng:** Writing – original draft, Validation, Supervision, Resources, Project administration, Methodology, Investigation, Funding acquisition, Conceptualization. **Jyoti R. Misra:** Writing – review & editing, Writing – original draft, Visualization, Validation, Supervision, Resources, Project administration, Methodology, Investigation, Funding acquisition, Formal analysis, Data curation, Conceptualization.

Declaration of competing interest

GZ is a co-founder of and has equity interest in Dialectic Therapeutics, which develops BCL-X_L PROTACs to treat cancer.

Acknowledgment

We would like to thank the Misra and Zheng laboratory members for their critical comments on the manuscript. We thank Dr. Shaun Olsen at UT Health Sciences Center San Antonio for the kind gift of 6xHis-CRBN/DDB1 complex and Dr. Girgis Obaid at University of Texas at Dallas for kindly allowing us to use the GelCount colony imager.

Appendix A. Supplementary data

Supplementary data to this article can be found online at https://doi.org/10.1016/j.heliyon.2024.e37829.

References

[1] A. Dey, X. Varelas, K.L. Guan, Targeting the Hippo pathway in cancer, fibrosis, wound healing and regenerative medicine, Nat. Rev. Drug Discov. 19 (2020) 480–494, https://doi.org/10.1038/s41573-020-0070-z.
[2] F.-X. Yu, B. Zhao, K.-L. Guan, Hippo pathway in organ size control, tissue homeostasis, and cancer, Cell 163 (2015) 811–828, https://doi.org/10.1016/j.cell.2015.10.044.
[3] M. Fu, Y. Hu, T. Lan, K.-L. Guan, T. Luo, M. Luo, The Hippo signalling pathway and its implications in human health and diseases, Signal Transduct. Targeted Ther. 7 (2022) 376, https://doi.org/10.1038/s41392-022-01191-9.
[4] J.R. Misra, K.D. Irvine, The Hippo signaling network and its biological functions, Annu. Rev. Genet. 52 (2018) 65–87, https://doi.org/10.1146/annurev-genet-120417-031621.
[5] A. Lopez-Hernandez, S. Sberna, S. Campaner, Emerging principles in the transcriptional control by YAP and TAZ, Cancers 13 (2021), https://doi.org/10.3390/cancers13164242.
[6] F. Zanconato, M. Cordenonsi, S. Piccolo, YAP and TAZ: a signalling hub of the tumour microenvironment, Nat. Rev. Cancer 19 (2019) 454–464, https://doi.org/10.1038/s41568-019-0168-y.
[7] Y. Wang, X. Xu, D. Maglic, M.T. Dill, K. Mojumdar, P.K. Ng, K.J. Jeong, Y.H. Tsang, D. Moreno, V.H. Bhavana, et al., Comprehensive molecular characterization of the Hippo signaling pathway in cancer, Cell Rep. 25 (2018) 1304–1317 e1305, https://doi.org/10.1016/j.celrep.2018.10.001.
[8] A. Kulkarni, M.T. Chang, J.H.A. Vissers, A. Dey, K.F. Harvey, The Hippo pathway as a driver of select human cancers, Trends Cancer 6 (2020) 781–796, https://doi.org/10.1016/j.trecan.2020.04.004.
[9] A. Dey, X. Varelas, K.-L. Guan, Targeting the Hippo pathway in cancer, fibrosis, wound healing and regenerative medicine, Nat. Rev. Drug Discov. 19 (2020) 480–494, https://doi.org/10.1038/s41573-020-0070-z.
[10] F. Zanconato, G. Battilana, M. Cordenonsi, S. Piccolo, YAP/TAZ as therapeutic targets in cancer, Curr. Opin. Pharmacol. 29 (2016) 26–33, https://doi.org/10.1016/j.coph.2016.05.002.
[11] F. Zanconato, M. Cordenonsi, S. Piccolo, YAP/TAZ at the roots of cancer, Cancer Cell 29 (2016) 783–803, https://doi.org/10.1016/j.ccell.2016.05.005.
[12] J.H. Park, J.E. Shin, H.W. Park, The role of Hippo pathway in cancer stem cell biology, Mol. Cell. 41 (2018) 83–92, https://doi.org/10.14348/molcells.2018.2242.
[13] C.D.K. Nguyen, C. Yi, YAP/TAZ signaling and resistance to cancer therapy, Trends Cancer 5 (2019) 283–296, https://doi.org/10.1016/j.trecan.2019.02.010.
[14] J. Miao, P.C. Hsu, Y.L. Yang, Z. Xu, Y. Dai, Y. Wang, G. Chan, Z. Huang, B. Hu, H. Li, et al., YAP regulates PD-L1 expression in human NSCLC cells, Oncotarget 8 (2017) 114576–114587, https://doi.org/10.18632/oncotarget.23051.
[15] B.S. Lee, D.I. Park, D.H. Lee, J.E. Lee, M.K. Yeo, Y.H. Park, D.S. Lim, W. Choi, D.H. Lee, G. Yoo, et al., Hippo effector YAP directly regulates the expression of PD-L1 transcripts in EGFR-TKI-resistant lung adenocarcinoma, Biochem. Biophys. Res. Commun. 491 (2017) 493–499, https://doi.org/10.1016/j.bbrc.2017.07.007.
[16] M.H. Kim, C.G. Kim, S.K. Kim, S.J. Shin, E.A. Choe, S.H. Park, E.C. Shin, J. Kim, YAP-induced PD-L1 expression drives immune evasion in BRAFi-resistant melanoma, Cancer Immunol. Res. 6 (2018) 255–266, https://doi.org/10.1158/2326-6066.CIR-17-0320.
[17] H.D. Huh, D.H. Kim, H.-S. Jeong, H.W. Park, Regulation of TEAD transcription factors in cancer biology, Cells 8 (2019) 600, https://doi.org/10.3390/cells8060600.
[18] K.C. Lin, H.W. Park, K.L. Guan, Regulation of the Hippo pathway transcription factor TEAD, Trends Biochem. Sci. 42 (2017) 862–872, https://doi.org/10.1016/j.tibs.2017.09.003.
[19] P. Chan, X. Han, B. Zheng, M. DeRan, J. Yu, G.K. Jarugumilli, H. Deng, D. Pan, X. Luo, X. Wu, Autopalmitoylation of TEAD proteins regulates transcriptional output of the Hippo pathway, Nat. Chem. Biol. 12 (2016) 282–289, https://doi.org/10.1038/nchembio.2036.
[20] J.K. Holden, J.J. Crawford, C.L. Noland, S. Schmidt, J.R. Zbieg, J.A. Lacap, R. Zang, G.M. Miller, Y. Zhang, P. Beroza, et al., Small molecule dysregulation of TEAD lipidation induces a dominant-negative inhibition of Hippo pathway signaling, Cell Rep. 31 (2020) 107809, https://doi.org/10.1016/j.celrep.2020.107809.
[21] J. Lou, Y. Lu, J. Cheng, F. Zhou, Z. Yan, D. Zhang, X. Meng, Y. Zhao, A chemical perspective on the modulation of TEAD transcriptional activities: recent progress, challenges, and opportunities, Eur. J. Med. Chem. 243 (2022) 114684, https://doi.org/10.1016/j.ejmech.2022.114684.
[22] E.R. Barry, V. Simov, I. Valtingojer, O. Venier, Recent therapeutic approaches to modulate the Hippo pathway in oncology and regenerative medicine, Cells 10 (2021) 2715, https://doi.org/10.3390/cells10102715.

[23] L. Hu, Y. Sun, S. Liu, H. Erb, A. Singh, J. Mao, X. Luo, X. Wu, Discovery of a new class of reversible TEA domain transcription factor inhibitors with a novel binding mode, Elife 11 (2022) e80210, https://doi.org/10.7554/eLife.80210.

[24] A. Gridnev, S. Maity, J.R. Misra, Structure-based discovery of a novel small-molecule inhibitor of TEAD palmitoylation with anticancer activity, Front. Oncol. 12 (2022), https://doi.org/10.3389/fonc.2022.1021823.

[25] K. Bum-Erdene, I.J. Yeh, G. Gonzalez-Gutierrez, M.K. Ghozayel, K. Pollok, S.O. Meroueh, Small-molecule cyanamide pan-tead·yap1 covalent antagonists, J. Med. Chem. 66 (2023) 266–284, https://doi.org/10.1021/acs.jmedchem.2c01189.

[26] T. Heinrich, C. Peterson, R. Schneider, S. Garg, D. Schwarz, J. Gunera, A. Seshire, L. Kötzner, S. Schlesiger, D. Musil, et al., Optimization of TEAD P-site binding fragment hit into in vivo active lead MSC-4106, J. Med. Chem. 65 (2022) 9206–9229, https://doi.org/10.1021/acs.jmedchem.2c00403.

[27] W. Lu, M. Fan, W. Ji, J. Tse, I. You, S.B. Ficarro, I. Tavares, J. Che, A.Y. Kim, X. Zhu, et al., Structure-based design of Y-shaped covalent TEAD inhibitors, J. Med. Chem. 66 (2023) 4617–4632, https://doi.org/10.1021/acs.jmedchem.2c01548.

[28] T.T. Tang, A.W. Konradi, Y. Feng, X. Peng, M. Ma, J. Li, F.-X. Yu, K.-L. Guan, L. Post, Small molecule inhibitors of TEAD auto-palmitoylation selectively inhibit proliferation and tumor growth of NF2-deficient mesothelioma, Mol. Cancer Therapeut. 20 (2021) 986–998, https://doi.org/10.1158/1535-7163.Mct-20-0717.

[29] T.A. Yap, D.J. Kwiatkowski, J. Desai, I. Dagogo-Jack, M. Millward, H.L. Kindler, A.W. Tolcher, S. Frentzas, A.W. Thurston, L. Post, et al., First-in-class, first-in-human phase 1 trial of VT3989, an inhibitor of yes-associated protein (YAP)/transcriptional enhancer activator domain (TEAD), in patients (pts) with advanced solid tumors enriched for malignant mesothelioma and other tumors with neurofibromatosis 2 (NF2) mutations, Cancer Res. 83 (2023) CT006, https://doi.org/10.1158/1538-7445.Am2023-ct006. CT006.

[30] A. Kaneda, T. Seike, T. Danjo, T. Nakajima, N. Otsubo, D. Yamaguchi, Y. Tsuji, K. Hamaguchi, M. Yasunaga, Y. Nishiya, et al., The novel potent TEAD inhibitor, K-975, inhibits YAP1/TAZ-TEAD protein-protein interactions and exerts an anti-tumor effect on malignant pleural mesothelioma, Am. J. Cancer Res. 10 (2020) 4399–4415.

[31] A.W. Tolcher, N.J. Lakhani, M. McKean, T. Lingaraj, L. Victor, M. Sanchez-Martin, K. Kacena, K.S. Malek, S. Santillana, A phase 1, first-in-human study of Ik-930, an oral TEAD inhibitor targeting the Hippo pathway in subjects with advanced solid tumors, J. Clin. Oncol. 40 (2022) TPS3168, https://doi.org/10.1200/JCO.2022.40.16_suppl.TPS3168. TPS3168.

[32] H. Shen, X. Xu, H. Rong, X. Song, J. Gao, J. Chen, D. Zhu, X. Zhao, J. Tong, Z. Zou, et al., Discovery of BPI-460372, a potent and selective inhibitor of TEAD for the treatment of solid tumors harboring Hippo pathway aberrations, Cancer Res. 83 (2023) 501, https://doi.org/10.1158/1538-7445.Am2023-501, 501.

[33] M. Fan, W. Lu, J. Che, N.P. Kwiatkowski, Y. Gao, H.-S. Seo, S.B. Ficarro, P.C. Gokhale, Y. Liu, E.A. Geffken, et al., Covalent disruptor of YAP-TEAD association suppresses defective Hippo signaling, Elife 11 (2022) e78810, https://doi.org/10.7554/eLife.78810.

[34] H. Hillen, A. Candi, B. Vanderhoydonck, W. Kowalczyk, L. Sansores-Garcia, E.C. Kesikiadou, L. Van Huffel, L. Spiessens, M. Nijs, E. Soons, et al., A novel irreversible TEAD inhibitor, SWTX-143, blocks Hippo pathway transcriptional output and causes tumor regression in preclinical mesothelioma models, Mol. Cancer Therapeut. (2023) OF1–OF11, https://doi.org/10.1158/1535-7163.Mct-22-0681.

[35] A. Fnaiche, H.-C. Chan, A. Paquin, N. González Suárez, V. Vu, F. Li, A. Allali-Hassani, M.A. Cao, M.M. Szewczyk, A. Bolotokova, et al., Development of HC-258, a covalent acrylamide TEAD inhibitor that reduces gene expression and cell migration, ACS Med. Chem. Lett. (2023), https://doi.org/10.1021/acsmedchemlett.3c00386.

[36] T. Lu, Y. Li, W. Lu, T. Spitters, X. Fang, J. Wang, S. Cai, J. Gao, Y. Zhou, Z. Duan, et al., Discovery of a subtype-selective, covalent inhibitor against palmitoylation pocket of TEAD3, Acta Pharm. Sin. B 11 (2021) 3206–3219, https://doi.org/10.1016/j.apsb.2021.04.015.

[37] H. Karatas, M. Akbarzadeh, H. Adihou, G. Hahne, A.V. Pobbati, E. Yihui Ng, S.M. Guéret, S. Sievers, A. Pahl, M. Metz, et al., Discovery of covalent inhibitors targeting the transcriptional enhanced associate domain central pocket, J. Med. Chem. 63 (2020) 11972–11989, https://doi.org/10.1021/acs.jmedchem.0c01275.

[38] K. Bum-Erdene, D. Zhou, G. Gonzalez-Gutierrez, M.K. Ghozayel, Y. Si, D. Xu, H.E. Shannon, B.J. Bailey, T.W. Corson, K.E. Pollok, et al., Small-molecule covalent modification of conserved cysteine leads to allosteric inhibition of the TEAD·Yap protein-protein interaction, Cell Chem. Biol. 26 (2019) 378–389.e313, https://doi.org/10.1016/j.chembiol.2018.11.010.

[39] Q. Li, Y. Sun, G.K. Jarugumilli, S. Liu, K. Dang, J.L. Cotton, J. Xiol, P.Y. Chan, M. DeRan, L. Ma, et al., Lats1/2 sustain intestinal stem cells and wnt activation through TEAD-dependent and independent transcription, Cell Stem Cell 26 (2020) 675–692.e678, https://doi.org/10.1016/j.stem.2020.03.002.

[40] Y. Sun, L. Hu, Z. Tao, G.K. Jarugumilli, H. Erb, A. Singh, Q. Li, J.L. Cotton, P. Greninger, R.K. Egan, et al., Pharmacological blockade of TEAD-YAP reveals its therapeutic limitation in cancer cells, Nat. Commun. 13 (2022) 6744, https://doi.org/10.1038/s41467-022-34559-0.

[41] M.R. Burke, A.R. Smith, G. Zheng, Overcoming cancer drug resistance utilizing PROTAC Technology, Front. Cell Dev. Biol. 10 (2022), https://doi.org/10.3389/fcell.2022.872729.

[42] A.C. Lai, C.M. Crews, Induced protein degradation: an emerging drug discovery paradigm, Nat. Rev. Drug Discov. 16 (2017) 101–114, https://doi.org/10.1038/nrd.2016.211.

[43] K. Li, C.M. Crews, PROTACs: past, present and future, Chem. Soc. Rev. 51 (2022) 5214–5236, https://doi.org/10.1039/D2CS00193D.

[44] D.A. Nalawansha, C.M. Crews, PROTACs: an emerging therapeutic modality in precision medicine, Cell Chem. Biol. 27 (2020) 998–1014, https://doi.org/10.1016/j.chembiol.2020.07.020.

[45] X. Sun, H. Gao, Y. Yang, M. He, Y. Wu, Y. Song, Y. Tong, Y. Rao, PROTACs: great opportunities for academia and industry, Signal Transduct. Targeted Ther. 4 (2019) 64, https://doi.org/10.1038/s41392-019-0101-6.

[46] M. He, C. Cao, Z. Ni, Y. Liu, P. Song, S. Hao, Y. He, X. Sun, Y. Rao, PROTACs: great opportunities for academia and industry (an update from 2020 to 2021), Signal Transduct. Targeted Ther. 7 (2022) 181, https://doi.org/10.1038/s41392-022-00999-9.

[47] M. Teng, N.S. Gray, The rise of degrader drugs, Cell Chem. Biol. 30 (2023) 864–878, https://doi.org/10.1016/j.chembiol.2023.06.020.

[48] B. Dale, M. Cheng, K.-S. Park, H.Ü. Kaniskan, Y. Xiong, J. Jin, Advancing targeted protein degradation for cancer therapy, Nat. Rev. Cancer 21 (2021) 638–654, https://doi.org/10.1038/s41568-021-00365-x.

[49] C. Cao, M. He, L. Wang, Y. He, Y. Rao, Chemistries of bifunctional PROTAC degraders, Chem. Soc. Rev. 51 (2022) 7066–7114, https://doi.org/10.1039/D2CS00220E.

[50] S.-L. Paiva, C.M. Crews, Targeted protein degradation: elements of PROTAC design, Curr. Opin. Chem. Biol. 50 (2019) 111–119, https://doi.org/10.1016/j.cbpa.2019.02.022.

[51] X. Liu, A. Ciulli, Proximity-based modalities for biology and medicine, ACS Cent. Sci. 9 (2023) 1269–1284, https://doi.org/10.1021/acscentsci.3c00395.

[52] C. Zhao, H. Wang, W. Zhan, X. Lv, X. Ma, Exploitation of proximity-mediated effects in drug discovery: an update of recent research highlights in perturbing pathogenic proteins and correlated issues, J. Med. Chem. 66 (2023) 10122–10149, https://doi.org/10.1021/acs.jmedchem.3c00079.

[53] M. Békés, D.R. Langley, C.M. Crews, PROTAC targeted protein degraders: the past is prologue, Nat. Rev. Drug Discov. 21 (2022) 181–200, https://doi.org/10.1038/s41573-021-00371-6.

[54] P.M. Cromm, C.M. Crews, Targeted protein degradation: from chemical biology to drug discovery, Cell Chem. Biol. 24 (2017) 1181–1190, https://doi.org/10.1016/j.chembiol.2017.05.024.

[55] M. Pettersson, C.M. Crews, PROteolysis TArgeting Chimeras (PROTACs) — past, present and future, Drug Discov. Today Technol. 31 (2019) 15–27, https://doi.org/10.1016/j.ddtec.2019.01.002.

[56] A. Gopalsamy, Selectivity through targeted protein degradation (TPD), J. Med. Chem. 65 (2022) 8113–8126, https://doi.org/10.1021/acs.jmedchem.2c00397.

[57] S.C. Rosenberg, F. Shanahan, S. Yamazoe, M. Kschonsak, Y.J. Zeng, J. Lee, E. Plise, I. Yen, C.M. Rose, J.G. Quinn, et al., Ternary complex dissociation kinetics contribute to mutant-selective EGFR degradation, Cell Chem. Biol. 30 (2023) 175–187.e115, https://doi.org/10.1016/j.chembiol.2023.01.007.

[58] D. Sun, J. Zhang, G. Dong, S. He, C. Sheng, Blocking non-enzymatic functions by PROTAC-mediated targeted protein degradation, J. Med. Chem. 65 (2022) 14276–14288, https://doi.org/10.1021/acs.jmedchem.2c01159.

[59] S. Montoya, J. Bourcier, M. Noviski, H. Lu, M.C. Thompson, A. Chirino, J. Jahn, A.K. Sondhi, S. Gajewski, Y.S. Tan, et al., Kinase-impaired BTK mutations are susceptible to clinical-stage BTK and IKZF1/3 degrader NX-2127, Science 383 (2024) eadi5798, https://doi.org/10.1126/science.adi5798.

[60] D. Chirnomas, K.R. Hornberger, C.M. Crews, Protein degraders enter the clinic — a new approach to cancer therapy, Nat. Rev. Clin. Oncol. 20 (2023) 265–278, https://doi.org/10.1038/s41571-023-00736-3.
[61] A.W. Konradi, T.T. Tang, Bicyclic Compounds, 2020. WO2020214734A1.
[62] M.S. Gadd, A. Testa, X. Lucas, K.H. Chan, W. Chen, D.J. Lamont, M. Zengerle, A. Ciulli, Structural basis of PROTAC cooperative recognition for selective protein degradation, Nat. Chem. Biol. 13 (2017) 514–521, https://doi.org/10.1038/nchembio.2329.
[63] W. Ji, W.S. Byun, W. Lu, X. Zhu, K.A. Donovan, B.G. Dwyer, J. Che, L. Yuan, X. Abulaiti, S.M. Corsello, et al., Proteomics-based discovery of first-in-class chemical probes for programmed cell death protein 2 (PDCD2), Angew. Chem. Int. Ed. 62 (2023) e202308292, https://doi.org/10.1002/anie.202308292.
[64] H. Li, Z. Ge, K. Lin, W. He, Q. Chu, M. Zheng, S. Zhang, T. Xu, Design, synthesis, and bioevaluation of transcriptional enhanced assocciated domain (TEAD) PROTAC degraders, ACS Med. Chem. Lett. 15 (2024) 631–639, https://doi.org/10.1021/acsmedchemlett.4c00029.
[65] S. Khan, X. Zhang, D. Lv, Q. Zhang, Y. He, P. Zhang, X. Liu, D. Thummuri, Y. Yuan, J.S. Wiegand, et al., A selective BCL-XL PROTAC degrader achieves safe and potent antitumor activity, Nat. Med. 25 (2019) 1938–1947, https://doi.org/10.1038/s41591-019-0668-z.
[66] P. Pal, D. Thummuri, D. Lv, X. Liu, P. Zhang, W. Hu, S.K. Poddar, N. Hua, S. Khan, Y. Yuan, et al., Discovery of a novel BCL-XL PROTAC degrader with enhanced BCL-2 inhibition, J. Med. Chem. 64 (2021) 14230–14246, https://doi.org/10.1021/acs.jmedchem.1c00517.